

https://dspace.org/

Vegetation and climate dynamics in a 16600year marine sequence offshore Mozambique in Delagoa Bight southeastern Africa

Frank Neumann; J Finch; A Hahn; C.S Miller; L Scott ...

https://hdl.handle.net/10539/46969
WOS

Downloaded from a DSpace repository. https://dspace.org/

Quaternary International 747 (2025) 109956

Contents lists available at ScienceDirect

Quaternary International

journal homepage: www.elsevier.com/locate/quaint

Vegetation and climate dynamics in a 16,600-year marine sequence offshore Mozambique in Delagoa Bight, south-eastern Africa

F.H. Neumann [a,b,c,d,*], J. Finch [c,e], A. Hahn [f], C.S. Miller [f,g], L. Scott [b], E. Schefuß [f], L. Dupont [h], H.C. Cawthra [i,j], F. Engelbrecht [k]

[a] Unit for Environmental Sciences and Management, North-West University, Potchefstroom, South Africa
[b] Department of Plant Sciences, University of the Free State, South Africa
[c] Discipline of Geography, School of Agricultural, Earth and Environmental Sciences, University of KwaZulu-Natal, South Africa
[d] Evolutionary Studies Institute, University of the Witwatersrand, Johannesburg, South Africa
[e] South African Environmental Observation Network (SAEON), Grasslands, Forests, Wetlands Node, Montrose, 3201, South Africa
[f] MARUM - Center for Marine Environmental Sciences, University of Bremen, Germany
[g] New College Bradford, Nelson St, Bradford, BD5 0DX, UK
[h] IJsselkade 21, Zutphen, the Netherlands
[i] Council for Geoscience, Cape Town, South Africa
[j] African Centre for Coastal Palaeoscience, Nelson Mandela University, South Africa
[k] Global Change Institute, University of the Witwatersrand, South Africa

ARTICLE INFO

Keywords:
Marine pollen record
Climate change
Anthropogenic impact
Southern Africa
Late Pleistocene
Mid-Holocene Altithermal

ABSTRACT

Few records of long-term vegetation dynamics and climate variability exist from coastal southeastern Africa. This study presents a new high-resolution marine pollen record (GeoB20615-2) from southern Mozambique, spanning the past *c.* 16,600 years. The chronology is based on a Bayesian age-depth model constructed using twelve radiocarbon dates on marine and terrestrial remains. Prior to *c.* 15,000 cal BP, pollen from ericaceous shrubs was prevalent, indicating low temperatures, while forest or woodland pollen taxa were minimal or absent. From *c.* 13,000 cal BP onwards, the record shows a gradual increase in savanna pollen taxa such as *Spirostachys* and *Burkea*, suggesting climatic warming. Pollen of *Spirostachys,* a woodland tree thriving in dry, warm regions, continues to increase into the early Holocene, between *c.* 11,200 and 9200 cal BP. After *c.* 9200 cal BP, a decline in *Spirostachys* pollen corresponds with a rise in *Podocarpus* pollen during a phase of high sea levels, indicating a potential expansion in coastal and/or montane forests, possibly reflecting increased moisture availability. From *c.* 3500 cal BP, *Podocarpus* pollen declines, likely due to more arid conditions, as indicated by a concomitant increase in Chenopodiaceae/Amaranthaceae, Asteraceae, and *Spirostachys* pollen. The youngest section of the profile is potentially affected by sediment mixing from *c.* 250 cal BP onwards. The section reveals the impact of European colonialists, with the appearance of neophytic pine pollen, and an increase in indigenous *Alchornea*, a disturbance indicator. The pollen results are in good agreement with terrestrial palynological records from the Indian Ocean Coastal Belt Biome such as Lake Eteza in northeastern South Africa. The GeoB20615-2 record contributes greater understanding of long-term vegetation dynamics and associated climatic shifts in the Indian Ocean Coastal Belt Biome.

1. Introduction

The coastal region of southeastern Africa is characterized by a diverse mosaic of forest, savanna, and wetland vegetation, shaped by summer rainfall, the Agulhas Current, and complex climate interplays (Intertropical Convergence Zone (ITCZ); South Indian Ocean Convergence Zone (SIOCZ); Reason, 2001; Zinke et al., 2004; Fig. 1). Current, and projected, climate change for southeastern Africa is expected to threaten ecosystem stability, biodiversity, and water availability in the region, under conditions of increasing temperatures leading to more

This article is part of a special issue entitled: Mapping Ancient Africa published in Quaternary International.

* Corresponding author. Unit for Environmental Sciences and Management, North-West University, Potchefstroom, South Africa.
E-mail address: Frank.Neumann@nwu.ac.za (F.H. Neumann).

https://doi.org/10.1016/j.quaint.2025.109956
Received 3 September 2024; Received in revised form 5 August 2025; Accepted 20 August 2025
Available online 29 August 2025
1040-6182/© 2025 The Authors. Published by Elsevier Ltd. This is an open access article under the CC BY-NC-ND license (http://creativecommons.org/licenses/by-nc-nd/4.0/).

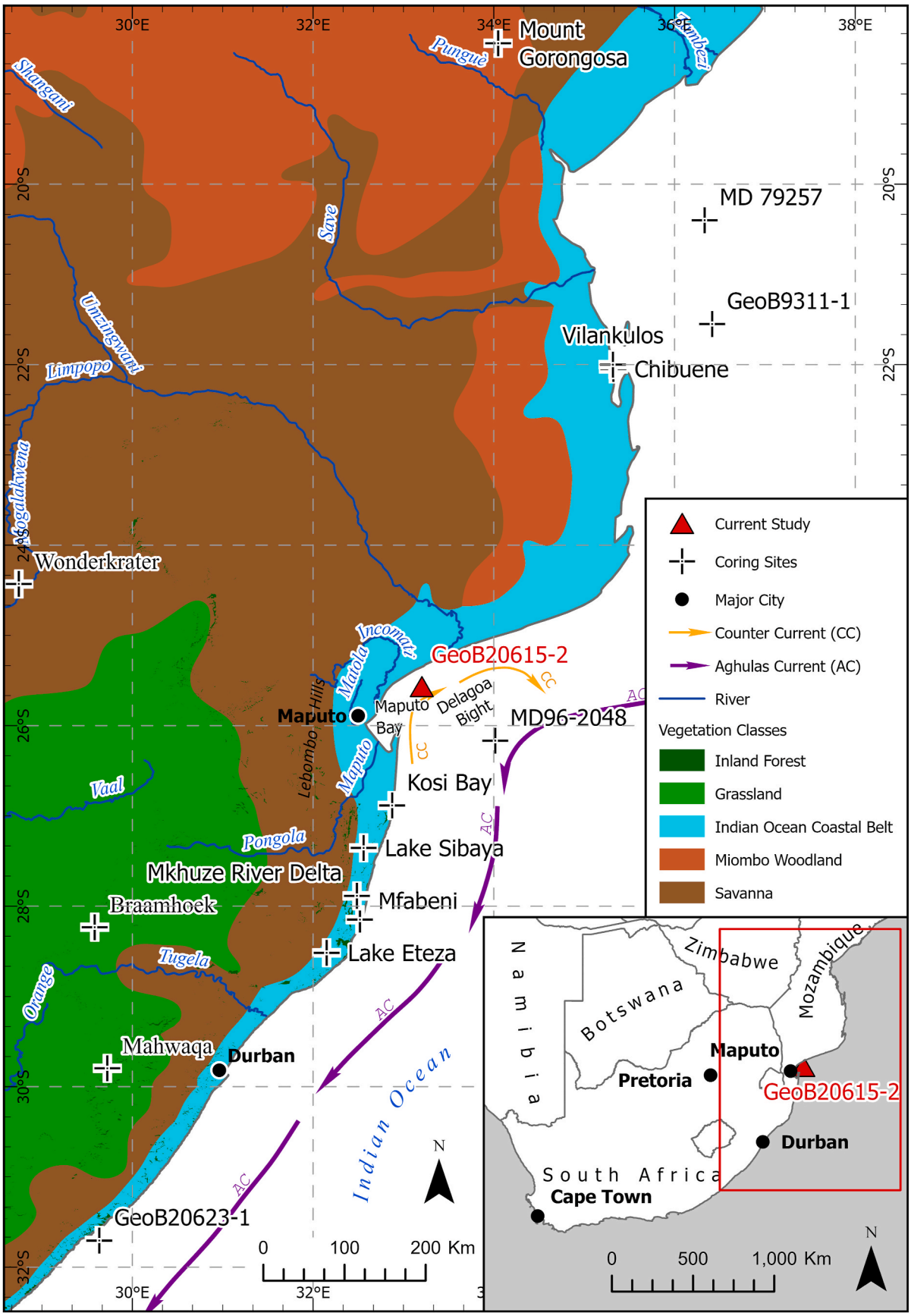


Fig. 1. Location of GeoB20615-2 relative to other key pollen studies and broad (biome-level) vegetation types (phytochoria) of southern Africa. Vegetation map is redrawn from Daru et al. (2016), which is based on White (1983) with modifications from Low and Rebelo (1996), Olson et al. (2001), Burgess et al. (2004) and Mucina and Rutherford (2006).

heatwave and fire-danger days (Engelbrecht et al., 2015). Uncertainty remains as to how these ecosystems are likely to respond to ongoing and anticipated climate changes, impacting biodiversity and communities who rely on the services they provide (see Scheffers et al., 2016). Long term records of past environmental change offer a unique lens on how ecosystems have responded to climate changes in the past, helping to better anticipate ecological responses to future environmental pressures in southeastern Africa (Niang et al., 2014; IPCC, 2021).

Unsurprisingly for a region typified by ecological and climatic diversity, palaeoclimatic reconstructions from across southern Africa indicate high spatial and temporal variability. Whereas the lack of organic rich sedimentary deposits limits progress in palaeoecology in the semi-arid landscapes of southern Africa (e.g. Scott et al., 2012), the humid coast of the Indian Ocean hosts deposits such as Lake Sibaya (Neumann et al., 2008), Lake Eteza (Neumann et al., 2010) and Mkhuze River Delta (Effiom et al., 2024), as well as the Mfabeni peatland that preserves a c. 50,000 years long pollen archive (Finch and Hill, 2008). Despite excellent pollen preservation along the coast, these records are often hampered by chronological issues (e.g., Lake Sibaya, Neumann et al., 2008; Mfabeni, Finch and Hill, 2008), limiting our understanding of how coastal vegetation responded to late Quaternary climate and sea-level change.

Late Quaternary palaeoclimate syntheses from the eastern summer rainfall region of southern Africa suggest spatial and temporal climatic variability across the subregion, with complex climate drivers at play (Scott et al., 2012; Chevalier and Chase, 2015). High latitude forcing was more dominant during MIS 3 and 2, with low-latitude insolation playing a greater role during the Holocene (Chevalier and Chase, 2015). Changing moisture availability is also closely linked to sea surface temperatures, which in turn are influenced by the strength of the warm Agulhas Current (e.g., at Lake Eteza, northern KwaZulu-Natal; Neumann et al., 2010).

Holocene-aged pollen records from the coastal zone of southeastern Africa reveal dynamic coastal vegetation that responded to climate shifts, with indications for human activity in the more recent past. Evidence from Lake Eteza (Neumann et al., 2010), the Mfabeni Peatland (Mazus, 2000; Finch and Hill, 2008), and Lake Sibaya (Neumann et al., 2008) shows that humid conditions during the Holocene Altithermal (*c.* 9000–6000 cal BP; Renssen et al., 2012; compare Partridge et al., 1999) promoted the spread of *Podocarpus*-dominated forests on the Maputaland coastal plain. The Lake Eteza record shows mid-Holocene *Podocarpus* forest expansion, due to wetter conditions and high sea levels (Neumann et al., 2010). This trend is reversed as climate became drier and sea levels retreated, indicated by increased Chenopodiaceae/Amaranthaceae and grass pollen (Neumann et al., 2010). Several records indicate a shift to drier savanna vegetation in the lake Holocene, indicative of continued drier conditions (e.g., Mkhuze River Delta, Effiom et al., 2024; Lake Sibaya, Neumann et al., 2008).

In southern Mozambique, shorter pollen records from coastal lakes and archaeological sites in Chibuene and Vilankulos offer insights into recent human interactions with the landscape (Ekblom, 2008; Ekblom et al., 2014a, 2014b). Pollen records from northeastern South Africa suggest increased human impact in the last few centuries (e.g., Neumann et al., 2008; Walther and Neumann, 2011). Despite these indications, palaeoecologists are limited in their ability to distinguish more subtle shifts in human activity, such as the influence of early farmers vs European colonists, due to the lack of high-resolution records and unequivocal pollen indicators from this region.

Here we present a 16,600-year-old marine pollen record (GeoB20615-2), supported by geochemistry and a radiocarbon chronology, from the Delagoa Bight, in Mozambique, a region sensitive to changes in temperature, rainfall, river discharge, and sea level change (Mavume et al., 2014; Dupont and Kuhlmann, 2017; Chevalier et al., 2020). Marine pollen records offer a regional climate and environmental perspective by averaging inputs across a broad catchment area, thereby reducing local bias often encountered in terrestrial records (Dupont and Kuhlmann, 2018). The GeoB20615-2 record is compared with sea-level data (Cooper et al., 2018), climate reconstructions (Chevalier and Chase, 2015), and the high-resolution terrestrial archive Lake Eteza (northeastern South Africa; Neumann et al., 2010) with the aim of understanding how coastal vegetation responded to climate forcing and sea-level change over time.

2. Regional setting

2.1. Topography, hydrology and Quaternary geology

The core site (GeoB20615-2) is located on the continental shelf *c.* 100 km northeast of Maputo, Mozambique, in the northern Delagoa Bight (Fig. 1) offshore of Maputaland (Fig. 1). The Maputaland coastal plain is up to *c.* 400 km wide (Förster, 1975), extends over c. 1200 km, and covers an area of >200,000 km^2 (Bruton and Cooper, 1980).

The location of Quaternary coastal plain deposits reflects a palaeotopographic influence during the marine transgressions and regressions of the Pleistocene (Botha, 2018). The adjoining offshore shelf is characterised by a northward-widening, steeply sloping margin with a shallow shelf break at *c.* 100 m. The Delagoa Bight Bay is tidally controlled with a shallow bathymetry (maximum water depth 30 m). The Limpopo River is the major river draining the surrounding region; however, it delivers little sediment to the core site because of an eastward deflection of the sediments by the cyclonic Delagoa Bight eddy (Preu et al., 2011; Schüürman et al., 2019). Most of the sediment arriving at the core site is delivered by three comparatively minor rivers: the (i) Incomati; (ii) Matola; and (iii) Maputo (Lusutfu)(Preu et al., 2011; Schüürman et al., 2019). These inputs fluctuate seasonally, with most of the freshwater discharges between November and April and a peak in January (Lencart e Silva et al., 2010).

2.2. Climate

Southern Mozambique receives summer rainfall. Average annual rainfall peaks along the coast at *c.* 1100 mm and decreases inland to *c.* 600 mm on the western plains (Van Wyk and Smith, 2001). At Delagoa Bight, average annual precipitation is *c.* 800 mm with common morning fog in winter (Siebert et al., 2004; Mavume et al., 2014). Maputaland has hot summers (average January temperature 27 °C) and cool to warm winters (average July temperatures of 16 °C) (Bruton and Cooper, 1980). Mean relative air humidity is high along the coast (55 % in August, 90 % in February).The climate of the coastal region of southern Mozambique is described as tropical savanna (tropical, savanna; mean monthly temperatures >18 °C, dry season, driest month <60 mm of precipitation and <4 % of total annual precipitation); classified as Aw following Köppen (1936) (Engelbrecht and Engelbrecht, 2016).

2.3. Vegetation

For the current study, we utilize the map of the broad (biome-level) vegetation types (phytochoria) of southern Africa by Daru et al. (2016) (Fig. 1). The map extends the phytogeographical map of Mucina and Rutherford (2006) beyond the borders of South Africa, Lesotho and Eswatini by implementing information from White (1983), with modifications and additions from Low and Rebelo (1996), Olson et al. (2001), and Burgess et al. (2004).

The locality of the core is adjacent to a coastal strip stretching from the south of Somalia to Gqeberha in the Eastern Cape of South Africa, termed Indian Ocean Coastal Belt Biome (IOCB), which has the highest woody plant species richness in southern Africa (White, 1983; Moll and White, 1978; Daru et al., 2016). The Maputaland coastal region that comprises southern Mozambique and the coast of KwaZulu-Natal, is a centre of plant endemism in southern Africa (Van Wyk and Smith, 2001) and forms part of the Maputaland-Pondoland-Albany biodiversity hotspot (Steenkamp et al., 2004). Mangrove swamps line the coast of

Mozambique, dominated by *Avicennia marina*, *Rhizophora mucronata*, and *Bruguiera gymnorrhiza* (Burrows et al., 2018).

The study site falls adjacent to the Indian Ocean Coastal Belt Biome (IOCB; Fig. 1). Miombo Woodland is prevalent further inland to the North of the Limpopo River (Fig. 1). The Grassland Biome is located further south, on the Highveld (Fig. 1), with restricted Forest Biome patches at higher altitudes. Each is described in detail in the following section.

2.3.1. Indian Ocean Coastal Belt Biome

The IOCB consists of two subunits, described as follows:

A. The Zanzibar-Inhambane Regional Mosaic of the IOCB is found North of the Limpopo River mouth, and comprises six forest types (Wild and Grandvaux Barbosa, 1967). These include evergreen, moist and dry forests, with the latter containing Mimosaceae, *Celtis africana*, *Ficus* spp., and *Adansonia digitata.* Other vegetation types include miombo-dominated woodland (*Brachystegia* spp., *Julbernardia globiflora*), bushland, littoral thicket with Combretaceae, *Mimusops afra* and *Manilkara discolor*, and grassland with palms and wetlands. This unit has floristic links to the Guineo-Congolian region and the Tongoland-Pondoland Regional Mosaic towards the south (Moll and White, 1978).
B. The Tongaland-Pondoland Regional Mosaic of the IOCB contains well-developed dune forest with canopy species such as *Mimusops afra*, *Euclea natalensis*, *Diospyros rotundifolia* and lianas such as *Rhoicissus* spp. Other forest taxa include *Celtis africana, Afrocarpus (Podocarpus) falcatus, P. latifolius, Manilkara discolor, Buxus macowanii, Mimusops obovate* and *Olea capensis* (Moll and White, 1978). Woodland with *Spirostachys africana* occurs along streams and on brackish flats (Burrows et al., 2018). Other vegetation types include thicket, bushland with palm veld (*Phoenix reclinata*, *Hyphaene natalensis*), grassland, a few fynbos genera (e.g., *Restio* spp.), and wetlands with *Cyperus papyrus*, *Eichhornia, Lemna* and *Potamogeton* (Moll and White, 1978).

2.3.2. Miombo Woodland

Miombo Woodland (*Brachystegia* spp., *Julbernardia*, Combretaceae) grows on well-drained, sandy soils (Burrows et al., 2018). The unit differs structurally and ecologically from the Savanna Biome, e.g., Mopane tree (*Colophospermum mopane*) communities in river valleys in drier regions or dry forests dominated by *Adansonia digitata*. *Senegalia* spp. and *Vachellia* spp. are widespread, *Spirostachys africana* grows along rivers, *Burkea africana* is an element of deciduous woodland, other trees such as *Pseudolachnostylis maprouneifolia* are adapted to e.g. sandy substrates (Burrows et al., 2018).

2.3.3. Forest Biome

Afromontane Forest Biome patches are located along the Lebombo Mountains (Fig. 1) and in central Mozambique, characterised by moderate endemism mostly among the trees (Mucina and Rutherford, 2006). Afromontane forest occurs mostly between 1200 and 2500 m a.s.l. where trees such as *Ilex mitis*, *Afrocarpus* (*Podocarpus) falcatus*, *Podocarpus milanjianus*, *Pittosporum viridiflorum*, *Olea capensis* and *Prunus africana* are abundant (Burrows et al., 2018). At higher altitudes >1200m, ericaceous bushland and montane grassland with *Erica* spp., often co-occurring with *Passerina montana*, *P. montivaga* and *Protea* spp., are widespread (Burrows et al., 2018). Along rivers and streams on high mountains in central Mozambique >1600 m a.s.l., ericoid shrubs such as *Cliffortia linearifolia, C. serpyllifolia* and *Leucosidea sericea* grow (Burrows et al., 2018). *Passerina rigida* is found on dunes in Maputo province (Burrows et al., 2018).

2.3.4. Grassland Biome

Grasslands are defined by a single layer of perennial herbaceous plants (mostly Poaceae), with woody vegetation restricted to areas protected from fire (Sell et al., 2024). Aside from the inland and mountainous areas where temperate Grassland Biome is distributed (Fig. 1), grasslands are often secondary. The secondary grassland remains open due to frequent burning, with only a few fire-resistant trees from the original vegetation persisting (Vesey-Fitzgerald, 1970; White, 1983; Chapman et al., 2001). While large tracts of vegetation in Maputaland remain near-pristine (van Wyk, 1994), human settlement has had a strong impact on grassland, forest, and especially the swamp forest ecosystems with its characteristic trees such as *Macaranga capensis, Voacanga thouarsi,* and *Raphia australis* (Felton, 1998; Burrows et al., 2018).

3. Materials and methods

3.1. Coring and lithology

Core GeoB20615-2 was collected on February 15, 2016 to the north of Delagoa Bight between the Limpopo and Incomati River mouths (25°33.073′S, 33°12.181′E, https://www.pangaea.de/expeditions/events/M123) (Fig. 1) during the M123 coring campaign of the German research vessel METEOR. The 532 cm-long core was extracted using a gravity corer from a water depth of *c.* 200 m. Core logging, including sediment colour, grain size, sediments structures and fossils, was done on board (Zabel, 2016). The core material is kept in cold storage at MARUM, University of Bremen. The subsampling strategy was as follows: (i) for palynology, 52 samples (5–12 g) were extracted at c. 10 cm resolution for pollen analysis; and (ii) for XRF, 139 samples were extracted at an average of 1 cm resolution for the upper 50 cm of the core, and a 5 cm resolution for the remainder of the core.

3.2. Radiocarbon dating

Twelve radiocarbon dates were obtained from the GeoB20615-2 core comprising a combination of planktonic foraminifera (5) gastropods (3) and terrestrial organic matter such as seeds (4). The sub-samples were taken throughout the core (between 2 and 355 cm) and were analysed at the radiocarbon laboratories in Poznan, Poland and the Alfred Wegener Institute, Bremerhaven, Germany (Table 1). These were calibrated using 'clam' (Blaauw, 2010) by applying the SHCal20 calibration curve (Hogg et al., 2020). For marine material a reservoir correction of ΔR of 121 ± 16 ^{14} C yr was applied (Maboya et al., 2017) (Table 1). The software Bacon (Blaauw and Christen, 2011) was used to calculate an age-depth model, which extrapolated the age-depth relationship for the sediments deposited from 352 to 532 cm (Fig. 2).

3.3. Sediment analyses-geochemistry

Discrete XRF analysis was performed on 124 sub-samples from sediment core GeoB20615-2 at MARUM, University of Bremen. Each sub-sample was first dried in an oven at 70 °C and then ground using a mechanical mill. XRF measurements for Al, Ca, Fe, K, Mg, and Si were carried out using a PANalytical Epsilon3-XL XRF spectrometer equipped with a rhodium tube, multiple filters, and an SSD5 detector. Quantification of element counts was achieved through calibration with certified standard materials (e.g., GBW07309, GBW07316, and MAG-1) following Govin et al. (2012). As elemental ratios are generally insensitive to dilution effects, we use the elemental ratios Fe/Ca, and K/Ti. The Fe/Ca ratio is widely used to trace changes in terrigenous input to marine deposits with high Fe indicating fluvial input while Ca represents the marine carbonate component (Govin et al., 2012 and references therein). The K/Ti ratio indicates weathering types since in climates with low chemical weathering rates K-rich illites are common clay minerals and the soil is concentrated in easily weathered elements such as K, stemming e.g. from feldspar. During intervals of humid climatic conditions, soils become depleted in water-soluble elements, such as K, which easily leach from the soils (Cohen, 2003; Croudace et al., 2015).

Table 1
Radiocarbon analyses from core GeoB20615-2. Ages calibrated with 'clam' (Blaauw, 2010) using the SHCal20 calibration curve (Hogg et al., 2020). Marine reservoir correction was based on Maboya et al. (2017). Calibrated mean ages are indicated.

Lab code	Depth (cm)	Material	14C age (BP)	Mean age (cal BP)	max95 %	min95 %	ΔR (^{14}C yr)
Poz-89103	2	Planktonic foraminifera	2300 ± 140	2165	2612	1804	121 ± 16
2115.1.1 AWI	20	Terrestrial material	1919 ± 75	1841	2034	1652	
2116.1.1 AWI	50	Terrestrial material	2415 ± 78	2512	2708	2334	
Poz-89104	52	*Globigerinoides ruber*	3780 ± 120	3997	4365	3667	121 ± 16
Poz-89105	102	*Globigerinoides ruber*	6400 ± 100	7176	7399	6948	121 ± 16
2117.1.1 AWI	152	Terrestrial material	4554 ± 354	5212	6083	4378	
Poz-89107	152	*Globigerinoides*	7410 ± 70	8106	8290	7977	121 ± 16
2118.1.1 AWI	202	Terrestrial material	8949 ± 99	10022	10265	9701	
Poz-89108	202	*Globigerinoides*	9080 ± 110	10042	10337	9686	121 ± 16
Poz-85015	277	Gastropods	13250 ± 60	15751	15947	15563	121 ± 16
Poz-89044	352	Gastropods	11360 ± 60	13153	13282	13085	121 ± 16
Poz-85017	355	Gastropods	11000 ± 60	12809	12942	12739	121 ± 16

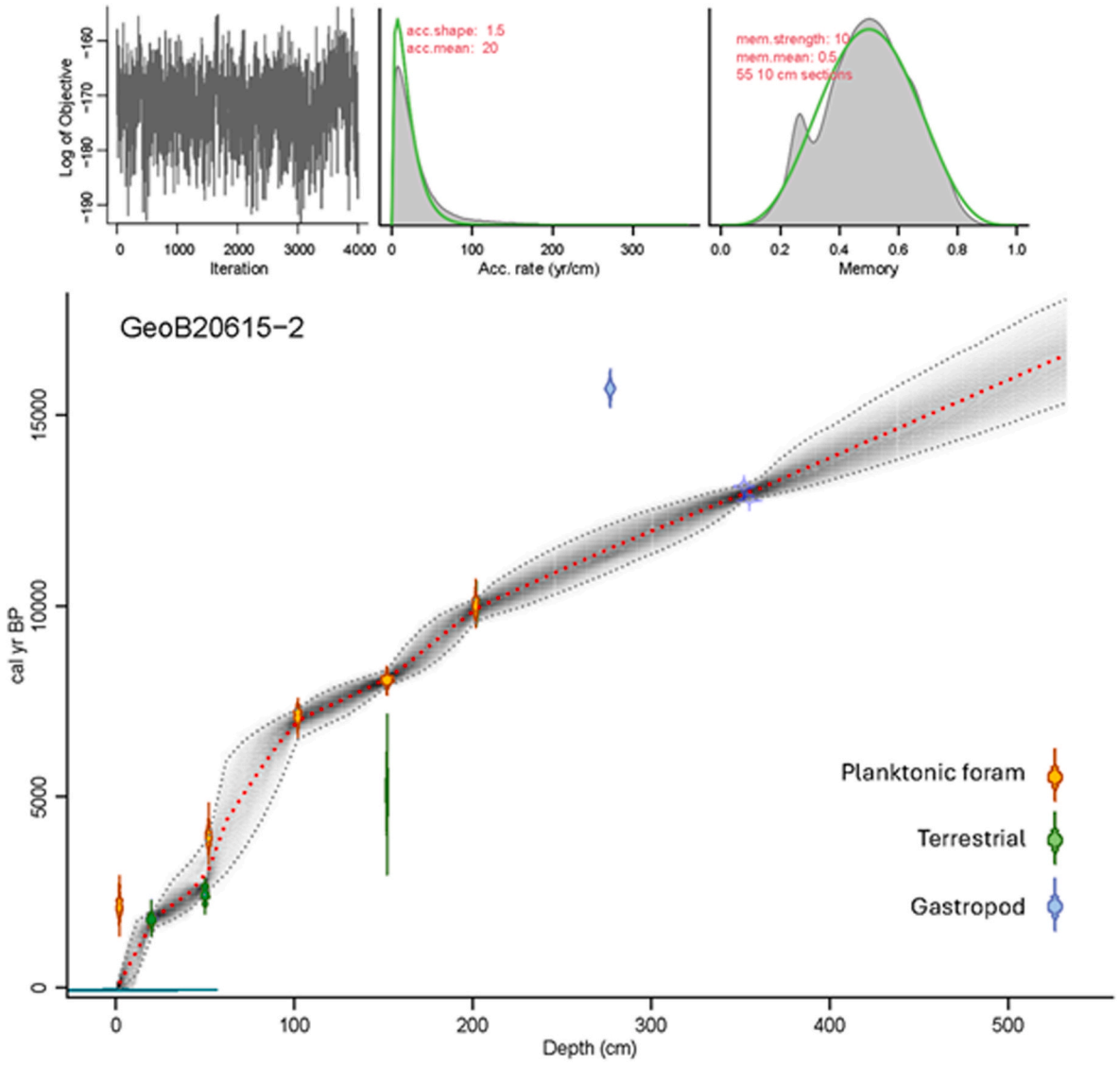


Fig. 2. Bayesian age-depth model (Bacon; Blaauw and Christen, 2011) based on samples from seeds, marine gastropods and planktonic foraminifera (Table 1). The section from 355 cm to the base is extrapolated. At 202 cm, the planktonic sample obscures a terrestrial one at the same depth.

In turn, the soils become enriched in insoluble elements such as Ti and the clay mineral smectite which is K depleted (Govin et al., 2012).

3.4. Palynology

Pollen samples were processed at the Department of Plant Sciences, University of the Free State (UFS). All subsamples were used up, but residues were retained. Fifty-two sub-samples, each weighing between 5

and 12 g, were prepared using a standard method with 10 % HCl, 10 % KOH, 40 % HF and acetolysis (Fægri and Iversen, 1989). The residues were further concentrated by heavy liquid mineral separation using ZnCl2 (specific gravity 2.0 g/l). Slides were mounted in glycerine jelly. Light microscopy (magnification 1000x, oil immersion) was applied at University of the Free State (UFS) (Zeiss Axioscope 5) and at the Evolutionary Studies Institute (ESI), University of the Witwatersrand (Olympus BX51).

Pollen identification was carried out to the lowest possible taxonomic level, supported by comparison with modern pollen reference collections at ESI and UFS and published pollen atlases such as Bonnefille and Riollet (1980) and Scott (1982). Pollen percentages were calculated based on the total number of pollen and spores with a sum of *c.* 200. The pollen data were plotted using Tilia 2.0 (Grimm, 1992) and the zonation was done by visual observation supported by stratigraphically constrained cluster analysis (total sum of squares; CONISS; Grimm, 1987).

4. Results

4.1. Lithology

The full core log for GeoB20615-2, published in Dyer et al. (2021), is summarized here. The basal layer of the sediment core at (532–510 cm) depth is composed of dark grey silty fine to medium sand with shell debris (see Zabel, 2016). From 510 to 416 cm depth, dark grey silty clay as well as bivalves, shell debris and mud clasts occur. From 416 to 232 cm, the sediments (clay to fine sand) darken, contain shell debris, and exhibit occasional bioturbation horizons and mud clasts. From 232 to 0 cm the sediments, composed of silty fine sand, are uniformly grey and rich in shell fragments, and from a depth of 88 cm upwards, contain foraminifera. The silty fine sand layer is intercalated at a depth of 23–21 cm with clay devoid of shell fragments.

4.2. Radiocarbon dating

Results of radiocarbon dating on twelve terrestrial and marine samples place the record in the late Pleistocene age range (Table 1). The Bayesian age-depth model is presented in Fig. 2 (Blaauw and Christen, 2011). The extrapolated section of the model between 355 and 532 cm suggests a basal age of *c.* 16,600 cal BP (Fig. 2). The Bayesian model designates three outliers which do not fall within the uncertainty envelope, *viz.* a marine gastropod age at 277 cm (13250 ± 60 14C BP; 15563–15947 cal BP), a terrestrial age at 152 cm (4554 ± 354 14C BP; 4378–6083 cal BP), and a foraminiferal age at 2 cm (2300 ± 140 14C BP; 1804–2612 cal BP) (Fig. 2; Table 1). Radiocarbon age estimates on terrestrial material were generally younger than planktonic foraminifera from similar depths, for example, the terrestrial outlier sample yielded an age of 4554 ± 354 14C BP (4378–6083 cal BP) with a large age uncertainty, whereas the marine foraminiferal age at the sample depth was *c.* 2000 years older (7410 ± 70 14C BP; 7977–8290 cal BP) (Table 1). Despite this general observation, marine and terrestrial ages at 202 cm depth yielded comparable results, with one sample obscuring the underlying sample on the age-depth model (Fig. 2; Table 1). The modelled age-depth relationship suggests that the record does not extend to the present day.

4.3. Sediment analyses-geochemistry

The main element for XRF analysis present in the sediment is Si (20–25 g/kg); secondary elements (>1 wt%) are Fe (55–81 g/kg), Ca (6–20 g/kg), and K (23–26 g/kg). Mn and Ti are minor (0.6–1.4 g/kg and 5–6 g/kg, respectively) (Fig. 3). The dry weight mass of the trace elements (Sr, Rb, Ni, V) is < 0.1 wt% (see Table S1). Fe/Ca ratios are higher in the lowermost 2.5 m than in the upper part of the core, the K/Ti ratio shows the opposite trend; except that values are relatively low in the upper 20 cm of the core as well as in the basal 2.5 m. The sediment accumulation rates (SAR) indicate a downward trend, with relatively higher SAR at the base of the core, decreasing towards the present day. Three brief periods of higher SAR are indicated, centred on *c.* 13,000, 7500 and 2500 cal BP.

4.4. Palynology

A pollen/spore sum of *c.* 200 was counted for most samples (pollen and spore sum: 65–277, median: 207), with at least two slides analysed per sample. The average temporal resolution of the sub-sampling is *c.* 319 years (52 sub-samples in 532 cm/*c.* 16,540 years of sediment accumulation (c. 31.5 yr/cm)). In total, 144 pollen and spore types, fungi and marine palynomorphs were identified. Pollen concentration was not calculated. Pollen and spore preservation was generally good, Varia (crumpled, corroded pollen grains that cannot be identified)

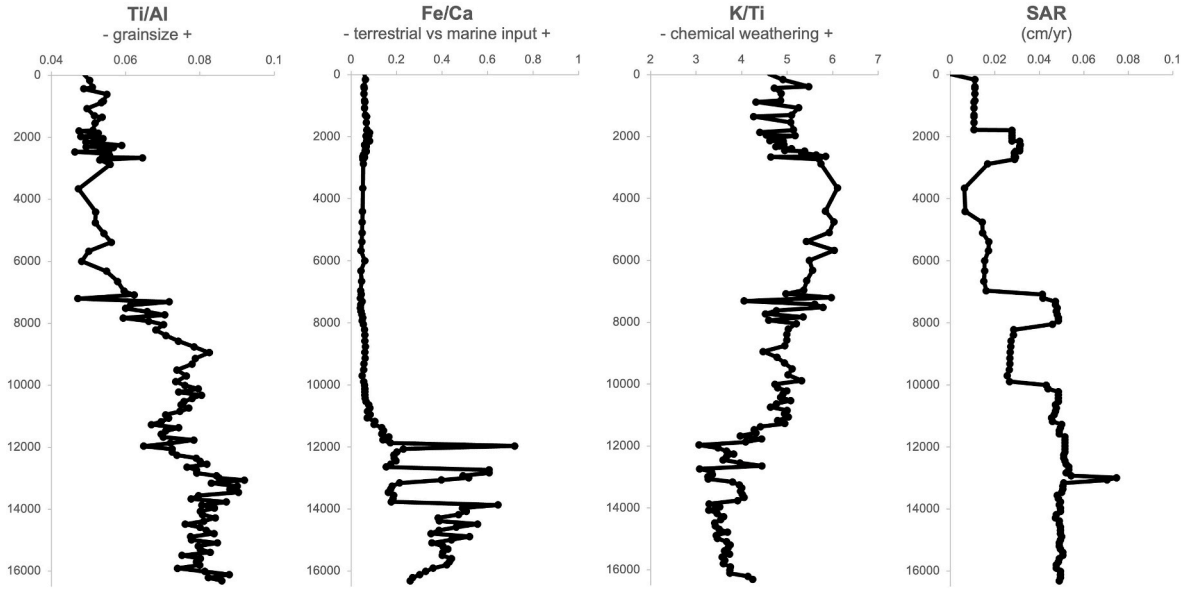


Fig. 3. Geochemical analyses of core GeoB20615-2. XRF data including Ti/Al, Fe/Ca, K/Ti and sediment accumulation rate (SAR).

counts are 0–5.1 %. Sixty-seven tree pollen types were observed, savanna trees included Miombo tree (*Brachystegia* sp.), Combretaceae, *Burkea* sp., and *Acacia*-type (contains *Senegalia* spp. and *Vachellia* spp., not differentiated here). Forest vegetation is reflected by pollen of the yellowwood tree *Podocarpus/Afrocarpus*, and coastal elements such as *Mimusops* spp., *Manilkara* sp., *Buxus* sp. and palms, especially *Phoenix* sp. Mangroves are represented by *Rhizophora* and *Bruguiera* sp. Forty-five pollen types of herbs and shrublets were identified. Alongside Poaceae, Asteraceae and Chenopodiaceae/Amaranthaceae, fynbos taxa such as Ericaceae and *Cliffortia* (termed ericaceous shrubs) were prominent in the bottom section of the profile (Fig. 4). Abundant wetland plants (Cyperaceae, *Typha*) and aquatics were recorded. Fern spores were sparse and low in diversity. Fungal spores, hyphae and fruit bodies were identified. Marine palynomorphs such as inner, organic linings of foraminifera, scolecodonts (mouthpieces of annelids) and dinoflagellate cysts were common, and especially the foraminiferal linings were in certain depths 10 times more abundant than all pollen and spores combined. In the current study dinoflagellate cysts were not differentiated.

Stratigraphically constrained cluster analysis (CONISS) defined four pollen assemblage and abundance zones (Bennett, 1996; Grimm, 1987) (Table 2, Fig. 4). Zone 4 is characterized by pollen of shrubby and fynbos vegetation such as Ericaceae and prominent grass and Cyperaceae components. Zone 3 is characterized by increasing pollen of mangrove elements such as *Rhizophora*, palms, woodland (*Olea*, forest and savanna elements) before pollen of grasses that were gradually declining,

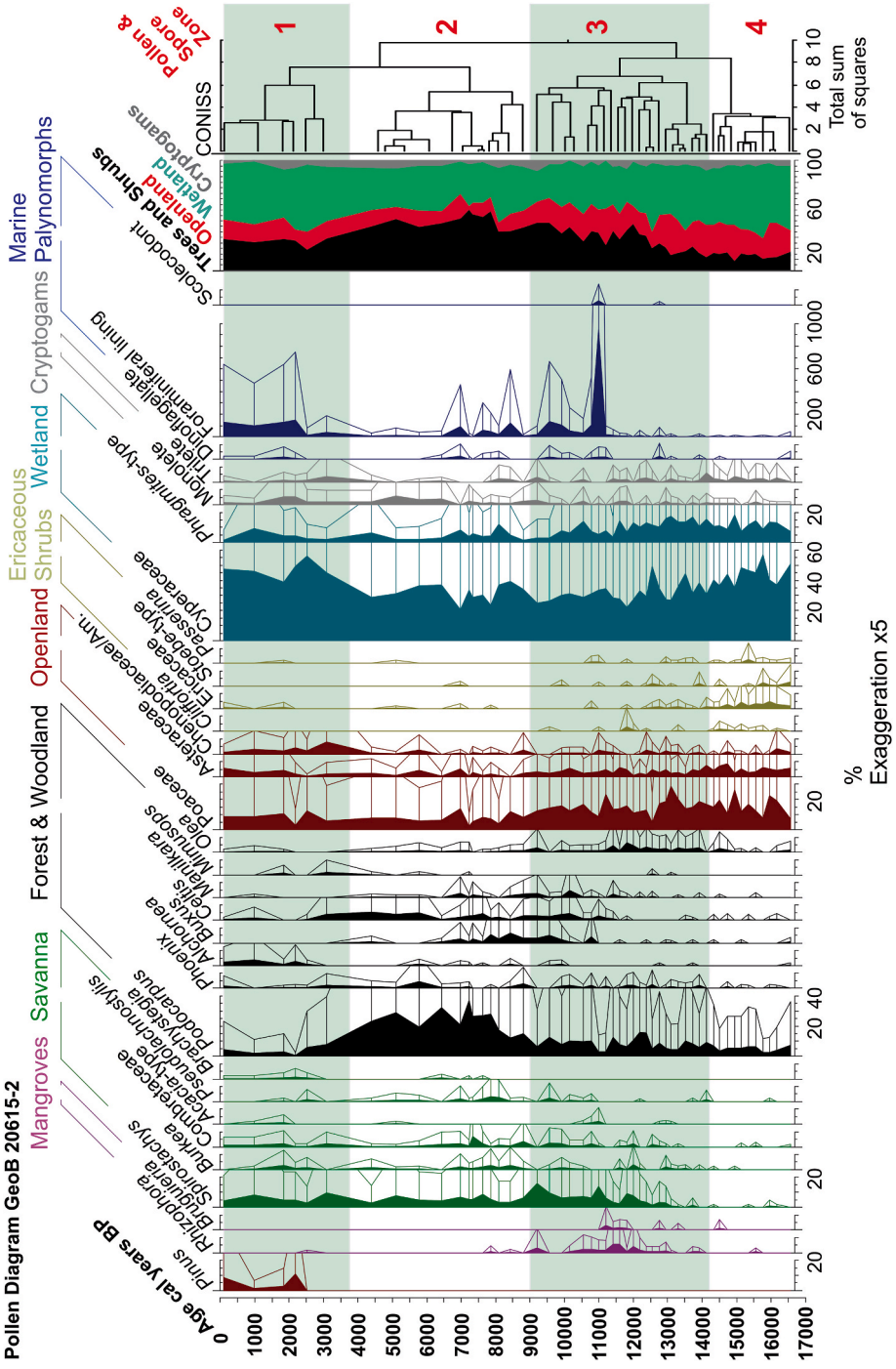


Fig. 4. Simplified pollen diagram of core GeoB20615-2 with stratigraphically constrained cluster analysis (CONISS-total sum of squares) and pollen zones.

Table 2
Pollen and spore zones of Geob20615-2.

Zone Name	Depth (cm)	Age (cal BP)	Sample Number	Period	Definition
Zone 1: *Pinus*–*Alchornea*–Amaranthaceae	57–0	c. 3700 – Present	6	Late Holocene	***Pinus* strong/exclusive to Zone 1:** 1–11 % ***Alchornea* prominent** **Rise in** Asteraceae & **Amaranthaceae** (8 %) Podocarpaceae & forest taxa decline (~3500 BP) Cyperaceae & marine palynomorphs increase
Zone 2: Podocarpaceae	177–57.1	c. 9000–3700	12	Mid - Late Holocene	**Podocarpaceae peak** (~40 %) Decline in Poaceae & *Phragmites*-type Strong *Buxus* presence in lower part
Zone 3: *Rhizophora*–*Olea*	407–177.1	c. 14200–9000	22	Pleistocene - Holocene transition	**Peak in *Rhizophora*** & *Bruguiera* (mangroves) ***Olea*** >6 % *Phoenix* prominent Podocarpaceae increasing *Spirostachys* up to 16 %
Zone 4: Ericaceae–Asteraceae	532–407.1	c. 16600–14200	12	Late Pleistocene	**Ericaceae peak** (~5 %) **High Asteraceae** & Poaceae (open land) Low Podocarpaceae (<10 %) Cyperaceae high: 57 - 31 %

dropped further in Zone 2. In Zone 2, representing the middle Holocene, Podocarpaceae pollen accompanied by other woodland elements increased. Finally in the late Holocene in Zone 1, Podocarpaceae pollen dropped and Asteraceae, Amaranthaceae and Cyperaceae pollen started increasing followed by a spread of exotic *Pinus* and indigenous *Alchornea* pollen while marine palynomorphs also became more prominent.

5. Discussion

5.1. Radiocarbon dating, the pinus pollen problem and depositional context

Pine pollen that appears in the top of the core at a depth of 30 cm (2000 cal BP, Fig. 2) seems to conflict with the age-depth model. Since pine trees are modern neophytes which were introduced by European settlers, their pollen could not have been deposited before *c.* 200 years ago (Neumann et al., 2008, 2010; Stager et al., 2013). To explain why *Pinus* pollen appears in sediments that are older than *c.* 200 years, we interpret that the uppermost section (30 cm) of the core contains sediments that were still in a liquid, un-consolidated state and prone to mixing. It is possible that as result of disturbance by coring activity, or during horizontal transport and storage, unconsolidated sediments from the top of the core contaminated sediments with modern pollen down to a depth of 30 cm. Any interpretation for this section is therefore tentative. In this case, pine pollen cannot be used as a reliable age indicator, as it was done in other terrestrial pollen studies in southern Africa (Stager et al., 2013).

If we assume a recent age for the top of the core, the planktonic foraminifera at the core top (2 cm depth) with a calibrated age of 2100 cal BP are too old, probably due to redeposition. This is corroborated by the age of the terrestrial material collected at 20 cm. Sediment redeposition is common in high-energy shelf environments, likely driven by the Agulhas Current and the Delagoa Bight eddy (Lamont et al., 2010). Another possible effect blurring age determination on foraminifera is bioturbation and differential dissolution. For example, on the Ontong Java Plateau, radiocarbon dating of coexisting planktonic foraminifera species and their shell fragments reveals age offsets up to *c.* 2200 years, attributed to the combined effects of differential dissolution, fragmentation, and bioturbation within the sedimentary mixed layer, as supported by steady-state modeling (Barker et al., 2007).

Core GeoB20615-2 was located on a slope seaward of the shelf break that experienced post-glacial marine transgression (Dyer et al., 2021). This is assumed to have caused the age reversal at the depth interval of 355–352 cm.

Since the ages below 355 cm are based on extrapolation, age estimations for the time between *c.* 16,600 and *c.*13,800 cal BP are less reliable than at younger levels. Consequently, the discussion of vegetation changes for this period, which is restricted to forest evolution, should be considered with caution when comparing with other palaeoarchives.

5.2. Palynology

5.2.1. Pollen taphonomy

Pollen and spore preservation in marine archives depends on air and water transport, pollen/spore dispersal traits, and post-depositional microbial as well as chemical degradation (Hamilton, 1972; Fægri and Iversen, 1989).

The success of a marine pollen study depends on how much taphonomic bias occurs during transport to the site (Havinga, 1967), that influences how well marine pollen reflects nearby continental vegetation. A good parameter for this is achieved by comparing the marine pollen archives to terrestrial sediment records with the aim of identifying regional vegetation trends (Dupont et al., 2007). A study on pollen in marine sediments offshore northwestern Africa showed clear links to continental vegetation zones and transport by winds and currents where key taxa reflect the position of these vegetation types demonstrating that marine studies can elucidate vegetation changes on land (Hooghiemstra et al., 2006). *Pinus* and *Podocarpus* pollen grains, like other buoyant, wind-transported conifer pollen, are often over-represented in marine/coastal sediments in relation to other taxa and must be interpreted with caution (Erdtman, 1957; Coetzee, 1967; Hamilton, 1972). Quantitative studies show that pollen is transported from vegetation to rivers and deposited in coastal marine sediments dependent on a variety of factors, such as water depths and buoyancy of pollen types (Chmura et al., 1999).

Pollen deposition along the Mozambican coast in the region of GeoB20615-2 is mostly fluvial, because winds mainly blow from the southeast limiting pollen transport from land (Lutjeharms, 2006; Dupont et al., 2011). Detrital sediment in the southern Maputo Bay originates from three rivers, the Incomati, Matola, and Lusutfu Rivers that flow into the Indian Ocean (Schüürman et al., 2019). The Limpopo River mouth is unlikely the main pollen source due to northward sediment drift in the counter current (Fig. 1; Schüürman et al., 2019). The 480 km long Incomati River drains 50,000 km^2 (Nakayama, 2003) and is probably the main source of the pollen and spores in GeoB20615-2. The Matola (Umbeluzi, Fig. 1), and Lusutfu (Maputo) rivers (Fig. 1), with catchments of *c.* 6600 km^2 respectively *c.* 22,700 km^2, are additional pollen

sources. A smaller catchment area is beneficial for interpreting marine records, as the terrestrial vegetation signal covers a smaller region. In a provenance study, Hahn et al. (2018) compared terrestrial material (pollens, plant lipids) from the Limpopo River catchment with coastal and shelf sediments across eastern Southern Africa and concluded that terrestrial signals in marine sediments generally reflect regional environmental gradients. In this case the influence of the Agulhas Current sediment distribution is only beyond the mid shelf, allowing reliable attribution of compositional changes in marine cores to environmental changes on land.

Differential pollen preservation can bias archives towards more degradation-resistant pollen e.g., Asteraceae and fern spores (Cushing, 1967; Hopkins and McCarthy, 2002). Pollen preservation is good in GeoB20615-2; no trend in the number of "Varia" pollen is observed. Notably, even in the anoxic soils of a mangrove swamp, pollen of mangrove taxa like *Rhizophora* and *Bruguiera* are rarely preserved (Phuphumirat et al., 2015; Sefton and Woodroffe, 2021). The good preservation of *Rhizophora* and *Bruguiera* pollen in GeoB20615 suggests that chemical alteration is negligible in this marine core setting. We propose that the palynomorph associations of our study can be reliably used to document changes in terrestrial vegetation.

5.2.2. Vegetation- and climate history in sedimentological context

5.2.2.1. Zone 4 (532-417 cm, c. 16,600–14,200 cal BP, 12 samples). The record dates to the late Pleistocene during the so-called Antarctic Cold Reversal (ACR) period when evidence from Antarctic ice cores reveals that the last deglaciation was interrupted by a millennial-scale cooling event, which occurred between 14,700 and 13,000 years ago (Pedro et al., 2016). Sedimentation started *c.* 16,600 cal BP with the deposition of fine sand (Fig. 4). At this time, sea level was *c.* 115 m lower than at present and the distance from the core site to the −115 m shoreline would have been *c.* 2 km. Cool climatic conditions are indicated by marked occurrence of Ericaceae which then gradually decline since *c.* 15,000 cal BP. This is in good agreement with very low temperatures based on peat brGDTGs (branched glycerol dialkyl glycerol tetraethers) from Mfabeni deposits at Lake St Lucia *c.* 16,000–15,000 cal BP (Fietz et al., 2023). Contemporary *Erica* spp. occurs in altitudes >1200 m a.s.l. in montane grasslands and forest margins in wet and cool habitats (Mucina and Rutherford, 2006; Burrows et al., 2018). *Cliffortia* spp., another ericoid shrub that grows along rivers in high altitude grasslands (Boon, 2010), appears regularly in Zone 4. Ericoid shrubs including *Cliffortia* and Ericaceae indicate cool, moist conditions at several inland sites during the late Pleistocene (*c.* 14,000 cal BP), including Wonderkrater, Mahwaqa Mountain, and Braamhoek (Scott, 2016; Scott et al., 2003; Neumann et al., 2014; Norström et al., 2014). The prevalence of ericoid shrubs during the late Pleistocene might be explained by lowering of the high-altitude ericaceous vegetation. Relatively low K/Ti ratios in GeoB20615-2 recorded during this interval indicate that weathering was mostly physical which corresponds with cooler, more arid climatic conditions (Fig. 3).

The forest pollen in Zone 4 partly represents the IOCB forest and woodland, while there is limited evidence for Miombo Woodland presence (*Brachystegia* spp., *Julbernardia globiflora*), which has a scattered distribution along the coast to just south of the Limpopo River (Moll and White, 1978). *Brachystegia* pollen is absent from Zone 4, savanna elements such as *Burkea* and Combretaceae are rare, pointing to a weak representation of savanna and Miombo woodland most probably due to low temperatures excluding frost-intolerant taxa. Coastal forest and woodland elements such as *Phoenix*, *Buxus*, *Celtis*, *Olea* and Sapotaceae (*Mimusops*, *Manilkara*), abundant in coastal forests (Moll and White, 1978), reach a minimum during this zone. Podocarpaceae are the dominant forest element in a largely open landscape with abundant Poaceae, Asteraceae, and Chenopodiaceae/Amaranthaceae but are less pronounced than in later periods. Widespread Podocarpaceae pollen in GeoB20615-2 might be partly due to overrepresentation in marine and terrestrial archives related to the bisaccate morphology as an adaptation to wind transport (Erdtman, 1957; Coetzee, 1967). *Afrocarpus* and *Podocarpus* pollen, both Podocarpaceae and morphologically similar, are not distinguishable when using light microscopy (Bamford et al., 2010). Since *Podocarpus latifolius* and *P. milanjianus* occur in montane regions, the Podocarpaceae pollen at GeoB20615-2 likely comes from *Afrocarpus falcatus*, which also grows in coastal and swamp forests of Maputo province (Eeley et al., 1999; Boon, 2010; Burrows et al., 2018). Podocarpaceae in coastal pollen records during the Pleistocene might not necessarily indicate permanent Afrotemperate forests in the coastal setting, but rather episodic migrations of podocarps from montane regions into swamp forests during favorable climatic periods (Mucina and Rutherford, 2006).

In Zone 4, locally wet conditions at GeoB20615-2 are indicated by a strong presence of Cyperaceae and *Phragmites*. *Phragmites australis* characterises humid zones within wetlands in southeastern Africa (Kotze and O'Connor, 2000). Marine palynomorphs are rare in Zone 4, consistent with a reconstruction of the palaeo-shoreline of the Delagoa Bight for the last *c.* 18,000 years (Mussa et al., 2003). Although the reconstruction does not include the location of core GeoB20615-2, it is assumed that the site was close to the shore *c.* 16,600–13,800 cal BP and the coast would be a curved embayment. High sedimentation rates and Fe/Ca ratios further indicate that grain size and fluvial input was high, suggesting a more proximal river mouth location and shorter transport pathway facilitating the deposition of coarse-grained riverine sediments (Fig. 3).

5.2.2.2. Zone 3 (417-177 cm, c 14,200 - 9000 cal BP, 22 samples). Podocarpaceae forests gradually spread at the beginning of Zone 3 during the late Pleistocene, together with drought-adapted but frost-sensitive *Spirostachys*. A decline in ericaceous shrubs, especially Ericaceae and *Stoebe*-type, indicates warmer conditions. The Mfabeni brGDGT record signals strong warming throughout the Pleistocene-Holocene transition (Fietz et al., 2023). At *c.* 13,000 cal BP, when climate amelioration is signalled both by decrease of ericaceous shrubs and the spread of forest, savanna and woodland elements, the temperature index at Wonderkrater in the savanna biome shows a first peak (Scott and Thackeray, 1987; Scott, 1982, 2016). This might indicate a short warming period even affecting localities further inland. Temperature indications have been obtained from pollen spectra from Wonderkrater and other sites in eastern South Africa (Scott, 1982, 2016, Scott and Thackeray, 1987; Scott et al., 2012; Chevalier and Chase, 2015; Thackeray et al., 2019; Chevalier et al., 2020). The Younger Dryas temperature reversal (12700–11600 cal BP), that followed the Allerød in the Northern Hemisphere (Raynaud et al., 2000), is not indicated in the GeoB20615-2 record, except maybe for the weak presence of fynbos pollen (Ericaceae, *Stoebe*-type), oscillating Podocarpaceae, fewer grasses and lower occurrence of woodland pollen (*Burkea*, Combretaceae, *Spirostachys*) (Fig. 4). Zone 3 is marked by the establishment of mangrove pollen (*Rhizophora* and *Bruguiera*) at *c.* 12,800–10,500 cal BP suggesting a major transgression that took place between *c.* 13,000 cal BP (65 m below sea level) and *c.* 8700 cal BP (15 m below sea level) (Cooper et al., 2018, Fig. 5).

Around 11,500 cal BP *Rhizophora* pollen decreased, and after *c.* 11,200 cal BP *Bruguiera* pollen no longer appears in GeoB20615-2, probably due to drowning of the mangal coastline during the transgression (Ellison, 1993; Tyson, 1995; Krauss et al., 2008).

The Holocene was characterised by marine inundation of coastal areas and regional rise in the coastal groundwater table (Mussa et al., 2003) (Fig. 5). At *c.* 11,000 cal BP strong marine influence GeoB20615-2 leads to the spread of dinoflagellates and scolecodonts, that, together with a peak in foraminiferal linings indicate greater water depth.

Since *c.* 11,000 cal BP, savanna and woodland elements gradually increase with a warming of the atmosphere (Simon et al., 2015) (Fig. 5).

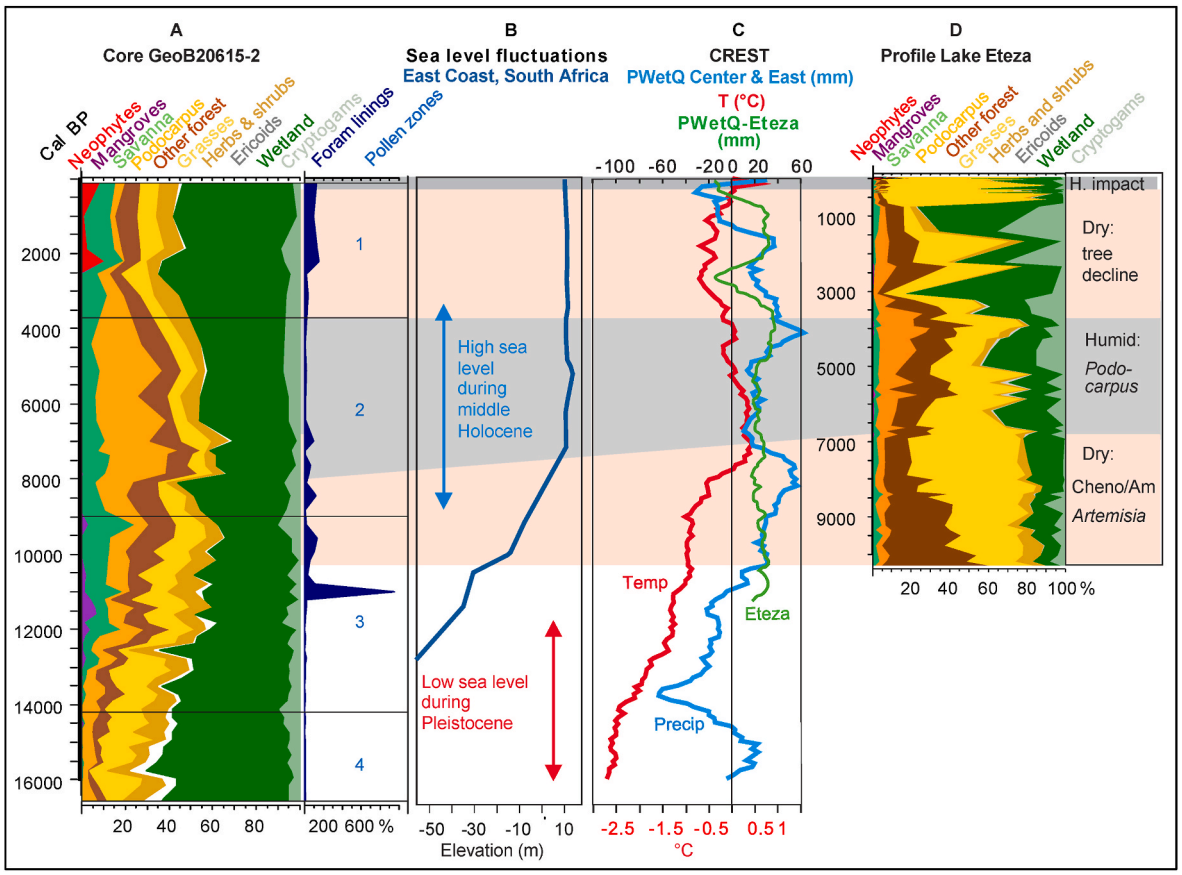


Fig. 5. Regional comparison eastern seaboard of southern Africa
A Stacked pollen diagram and microforaminiferal linings of core GeoB20615-2 (this study), Podocarpac.-Podocarpaceae
B Sea level fluctuations at the eastern coast of South Africa (Cooper et al., 2018)
C PWetQ Center and East, precipitation of the wettest quarter, centre and eastern precipitation stack was calculated based on reconstructions from Braamhoek, Equus Cave, Blydefontein, Florisbad, Mfabeni wetland and Lake Eteza. TmeanAnn, reconstructed variables of the mean annual temperature based on reconstructions from 11 sites from the summer rainfall region of South Africa (Chevalier and Chase, 2015). Uncertainties not shown.
D Stacked pollen diagram of Lake Eteza (Neumann et al., 2010), Podocarpac.-Podocarpaceae. H. impact = Human impact.

Savanna trees such as *Burkea africana*, Combretaceae and *Senegalia/Vachellia* spp., together with elements of coastal dune forest (Coates-Palgrave, 2002), spread (Fig. 4). This indicates that the coring location was close to a dune forest as the sea level *c.* 10,000 cal BP was −30 m lower than today and rapidly increased by 10 m within 1000 years (Cooper et al., 2018, Fig. 5). During this time, barrier islands developed along the northern coast. De Lecea et al. (2017) reveal the development of shorelines that enclosed parts of Bay resulting in morphological forcing of the back barrier. A palaeo-shoreline at −20 m, with associated enclosing lagoons developed, now drowned by rising sea levels. A high water table might be responsible for the strong occurrence of wetland taxa including Cyperaceae and *Phragmites*, although those taxa gradually decrease when the forest spreads in the pollen record (Fig. 4). The increase of forest, savanna and woodland elements is also reflected by the gradual decrease of open land indicators, especially Asteraceae and Poaceae since *c.* 10,000 cal BP at GeoB20615-2 (Fig. 4).

A moderate spread of forest elements, e.g., *Olea* (prominent until *c.* 11,000 cal BP and then declining due to the spread of more warmth-demanding taxa), *Phoenix* as an element of palm veld along the coast, *Celtis* and *Manilkara*, can be linked to warm, humid conditions. Pollen of *Spirostachys* increases until the top of Zone 3 at *c.* 9200 cal BP suggesting warm, dry conditions (Boon, 2010).

5.2.2.3. Zone 2 (177-57 cm, c 9000 - 3700 cal BP, 12 samples). Since *c.* 9000 cal BP, at the beginning of Zone 2, the modern Maputo Bay formed together with the emergence of further barrier islands (De Lecea et al., 2017). During the same time, pollen of Poaceae and Asteraceae gradually retreated at GeoB20615-2, an effect of the spreading forest vegetation, especially Podocarpaceae, whereas pollen of wetland taxa are equally strongly represented as compared with Zone 3. A strong sea level increase is accompanied by high SSTs which might have led to an increase in precipitation (Bard et al., 1997). Further regional SST records (Wang et al., 2015 - UK37 record) indicate that SSTs remained stable over the past *c.* 8000 years. *Brachystegia* pollen, indicating coastal Miombo Woodland close to the coring site, appears at *c.* 7500 cal BP and vanishes from the pollen record at *c.* 6000 cal BP (Fig. 4). The inlet probably breached dune corridors along the coast, which might explain why, together with the spread of *Podocarpus* (maybe *Afrocarpus falcatus*) which marks Zone 2, dune forest elements such as *Buxus* and *Manilkara*, were gradually declining until *c.* 6500 cal BP at GeoB20615-2. Mangroves are largely absent from the pollen record after *c.* 7600 cal BP at GeoB20615-2 which might also be connected to the formation of Maputo Bay (Mussa et al., 2003). During the middle Holocene (*c.* 7000–3600 cal BP), high sea levels, increased precipitation and elevated water table created humid conditions that supported forest expansion -particularly *Podocarpus*-at Lake Eteza and GeoB20615-2 (Neumann et al., 2010; Cooper et al., 2018, Fig. 5). The dominance of Podocarpaceae in Zone 2 during the Mid-Holocene Altithermal is marked by a peak at *c.* 7000 cal with >35 %. This matches the Mfabeni pollen record, where Podocarpaceae spread after *c.* 8000 cal BP (Finch and Hill, 2008). The later spread of forest at Mfabeni might suggest delayed onset of warm and humid Mid Holocene conditions further south or may be due

to chronological uncertainties in the Mfabeni record. At GeoB20615-2, a strong marine influence is indicated by continuously high, but strongly fluctuating, percentages of dinoflagellate cysts and foraminiferal linings until *c.* 7000 cal BP. Then marine palynomorphs decrease slightly at GeoB20615-2 (Fig. 4), possibly owing to more stable sea levels (Cooper et al., 2018).

It is possible that because of the substantial spread of Podocarpaceae, savanna and woodland elements such as Combretaceae and *Pseudolachnostylis* slowly retreat until *c.* 5000 cal BP. Under the very humid conditions, fire-sensitive Podocarpaceae seemed more competitive than savanna taxa which might be explained by fire suppression under high rainfall conditions (Adie et al., 2017). The modern sedimentary environment of Delagoa Bight, including Inhaca Island, probably evolved between *c.* 7000–5000 cal BP, with the bay becoming more stable (Mussa et al., 2003). Estuarine sediments from Macassa Bay south of Vilankulos indicate higher sea levels between *c.* 6600 and *c.* 6300 BP based on the presence of marine diatoms and supporting magnetic susceptibility data (Norström et al., 2012). Geomorphological evidence from the barrier islands Inhaca and Bazaruto indicates that the mid-Holocene high sea-level period started after *c.* 6000 ± 300 cal BP and ceased by *c.* 3700 cal BP (Armitage et al., 2006), *c.* 1000 years later than indicated in the Cooper et al. (2018) record. These changes in coastal topography would have triggered substantial changes in the pollen and spore spectra of GeoB20615-2, mainly the drastic drop of Podocarpaceae since *c.* 5000 cal BP (Figs. 4 and 5). In addition, a suggested decrease in precipitation would have influenced vegetation (compare Neumann et al., 2010). Cyperaceae and eventually, Chenopodiaceae/Amaranthaceae (as a halophytic element, probably growing at the coast), spread at the transition to Zone 1 at *c.* 3200 cal BP.

Relative to the preceding zones, the K/Ti ratio in Zone 2 is high, indicating that more chemical weathering took place during overall wetter climatic conditions.

5.2.2.4. Zone 1 (57-2 cm, c. 3200 - 108 cal BP, 6 samples). During the late Holocene in Zone 1, a decrease of Podocarpaceae and trees such as *Celtis* and *Mimusops*, as well as an increase of dry indicators Asteraceae and Chenopodiaceae/Amaranthaceae and to a lesser degree grasses, coincide with a return to lower sea levels (Figs. 4 and 5). During the last *c.* 2700 years marine palynomorphs, especially foraminiferal linings but also dinoflagellate cysts, become more prominent.

K/Ti values decline relative to Zone 2 (Fig. 3), indicating reduced chemical weathering under drier conditions, possibly explaining the forest pollen decline in GeoB20615-2. Similar observations at Lake Eteza suggest comparable vegetation and climate patterns across both sites and possibly along the Indian Ocean coast (Neumann et al., 2010).

During the same time, increasing Cyperaceae pollen reached an absolute maximum at *c.* 2200 cal BP at GeoB20615-2. The retreat of forests and the low sea level might have favored the advance of sedge-dominated wetlands closer to the coring site.

Alchornea, growing in coastal forest understorey e.g. in Central Africa where it indicates anthropogenic disturbance (Mercuri et al., 2018), became prominent during the last *c.* 2600 years in the current study (Fig. 4). *Pinus*, a neophyte, occurs during the last *c.* 200 years in southeastern Africa, planted by European settlers, as indicated for the Lake Sibaya pollen record (Neumann et al., 2008).

At GeoB20615-2, *Pinus* pollen appears at *c.* 2200 cal BP, which conflicts with the introduction of *Pinus* to the region and can, as explained above, be due to bioturbation or modern contamination during the coring process (see 5.1). The vegetation history of the last *c.* 2200 years, encompassing the emergence of Early Farming Communities and their potential impact on the landscape (see Neumann et al., 2008; Olatoyan et al., 2022), is consequently not robust for GeoB20615-2. This is due to the above-mentioned contamination/disturbances and a very low resolution of only three samples which might also be a result of a low sedimentation rate at the top of the core. The last *c.* 2200 years at GeoB20615-2 are further characterised by a decline of forest taxa including Podocarpaceae, a spread of Miombo (*Brachystegia*) woodland and an increase in acacias (*Senegalia/Vachellia)*.

5.3. Regional forest development at the Indian Ocean coast

5.3.1. General forest dynamics-Quaternary

The pollen record from GeoB20615-2 reflects forest evolution along the Indian Ocean coast since the Late Pleistocene impacted by complex fluctuations of sea levels and climate (Fig. 5). The marine archive reflects a dynamic interplay between fire-prone subtropical savanna and IOCB taxa and moisture-dependent Afrotemperate forest trees, particularly *Podocarpus* (Figs. 4 and 5). Afromontane forests are situated at higher altitude and exposed to markedly seasonal climates (Lawes et al., 2000a, 2000b), whereas IOCB forests grow at the Indian Ocean in a stable climate. Afromontane forests are more patchy than coastal forests, which form an almost continuous belt along the eastern coast of South Africa on dunes (Lawes et al., 2007). IOCB forests in South Africa were established after the Last Glacial Maximum when a new dune cordon allowed subtropical flora to migrate southwards together with the southward shift of the ITCZ (Mucina et al., 2006).

Afrotemperate forest taxa such as *Podocarpus* expanded under temperate or warm high rainfall conditions, low seasonality and reduced fire frequency, often persisting in fire refugia like rocky outcrops (Adie et al., 2017). In contrast, subtropical savanna and coastal taxa thrived under warm, drier, more seasonal climates with frequent fires, which limited forest spread and favored fire-adapted species with a savanna-affiliation (Lawes, 1990; Eeley et al., 1999; Adie et al., 2017; Beckett and Bond, 2019; Effiom et al., 2025). Afrotemperate taxa growing within the IOCB today are exclusive to swamp forests (Venter, 1972; Lubbe, 1997; Mucina and Rutherford, 2006). Afromontane forests were probably evolutionarily older than IOCB plant communities (Eeley et al., 1999). Lawes et al. (2000a) suggest that palaeoclimatic events had a greater impact on Afromontane forests because they are much older than the Last Glacial Maximum and have experienced more than one extinction filtering event, unlike the younger IOCB forests.

5.3.2. Forest evolution since the Late Pleistocene: a regional comparison

Comparison of forest evolution throughout the late Quaternary at Lake Eteza (for the last c. 10,200 years, Neumann et al., 2010, Fig. 5) and GeoB20615-2 (for the last 16600 years, Figs. 4 and 5) allow a detailed investigation of similar trends along the Maputaland coast. GeoB20615-2, despite moderate resolution and chronological uncertainties, reflects crucial vegetation changes at the Late Pleistocene-Holocene transition. Foraminifera linings and dinoflagellate cysts provide important insights into the role of sea level as a driver of regional vegetation change including the occurrence of Ericaceae pollen pointing to lower temperatures as evidenced also at inland records (Botha et al., 1992; Scott, 1982, 2016; Scott et al., 2012; Chevalier and Chase, 2015). Here the advantage of a broad catchment area and the possibility of deducing marine influence are advantageous in the offshore record. Amongst the pollen records from southeastern Africa along the coast of the Indian Ocean (Finch and Hill, 2008; Ekblom, 2008; Ekblom et al., 2014b; Dupont and Kuhlmann, 2018), Lake Eteza, located to the South of the Mfolozi floodplain *c.* 25 km away from the coast within the IOCB (Neumann et al., 2010), has the most reliable resolution and chronology for intercomparison with GeoB20615-2. The lake is surrounded by grassland with palm veld, coastal dune forest, and mangroves at the St Lucia estuary. In the interior savanna, along the escarpment, scarp forests occur (Neumann et al., 2010). All these biomes are reflected in the pollen record and enable comparison with GeoB20615-2 (Fig. 2). Sea-level fluctuations (Cooper et al., 2018, Fig. 2) affect vegetation through changes of the water table, marine ingressions, erosion and possible drowning of mangrove forest during marine transgressions.

Since *c.* 16,600 cal BP until the late Pleistocene in Zone 4, grasses and

ericaceous shrub elements at GeoB20615-2 indicated open vegetation under cool climatic conditions, influenced by low sea levels (<−50m) (Fig. 5). From *c.* 12,700 cal BP until *c.* 9000 cal BP the subtropical arboreal vegetation of the IOCB was established with (sub)tropical trees whereas Ericaceae decreased along with atmospheric warming and an increase of humidity (Fig. 5; Mucina et al., 2006). Between *c.* 12500 and *c.* 11,000 cal BP a mangrove peak is recorded at GeoB20615-2 (Fig. 4). As the rapid post-glacial marine transgression continued, reaching −30 m at *c.* 11,000 cal BP, marine influence reached the threshold necessary for mangroves to establish at the Delagoa Bight coast. At *c.* 11,000 cal BP a sudden sharp increase of micro-foraminiferal linings, which were until then nearly absent from the GeoB20615-2 pollen record, shows a stronger marine influence at the coring site which is mirrored by rising sea levels (Fig. 2). Until *c.* 10,000 cal BP, with a continued rise in sea level, mangrove retreats. At Lake Eteza (Neumann et al., 2010), a similar pattern of vegetation changes is observed in comparison to the GeoB20615-2 palynological record until *c.* 8700 cal BP. Lake Eteza shows high forest pollen percentages and a retreat of grasses at *c.* 9000 cal BP (Fig. 5).

From the Mid-Holocene Altithermal until the Late Holocene, from *c.* 8000–3600 cal BP, it was generally humid at both Lake Eteza and GeoB20615-2, which is indicated by high percentages of Podocarpaceae pollen. This might show a high influence of a strong Afrotemperate forest element (probably *Afrocarpus falcatus*) in the coastal forests. The period between *c.* 8000 and 7500 cal BP shows a peak in reconstructed precipitation (PWetQ) for the central and eastern region (Chevalier and Chase, 2015). Curiously, the time between *c.* 8000–6800 cal BP is rather dry at Lake Eteza whereas a Podocarpaceae peak is obvious (parallel to GeoB20615-2) at *c.* 6800–3800 cal BP (Fig. 2). Judging from the earlier spread of *Podocarpus* in GeoB20615-2 at *c.* 8000 cal BP than in Eteza at *c.* 7000 cal BP, the forests appear to have spread along the coast from north to south.

Around 8000 cal BP, MD79257 shows a short-term decline of SSTs which coincides with a mangrove and forest tree decline in GeoB20615-2, coupled with a spread in wetland elements (Bard et al., 1997). A similar fluctuation is absent at Lake Eteza (Neumann et al., 2010). At GeoB20615-2, Podocarpaceae percentages *c.* 7500–4500 cal BP reach a maximum, signalling moist conditions. This coincides with peak SSTs (nearly 28 °C) and maximum sea level in the Mozambique Channel during the Holocene (Fig. 5). During the Mid-Holocene Altithermal, the high-pressure cells were displaced poleward, and the easterlies could bring tropical moisture to the region (Hahn et al., 2017). *Podocarpus* expanded along the Indian Ocean coast of southern Africa, as shown at GeoB20815-2, Lake Eteza, Lake St Lucia, Mkhuze River delta and Mfabeni (Neumann et al., 2010; Effiom et al., 2024, 2025; Finch and Hill, 2008) (Fig. 5). This expansion is likely linked to warmer and more humid conditions, enhanced monsoonal activity, and a stronger Agulhas Current, which increased coastal rainfall (Neumann et al., 2010). These conditions reduced fire frequency and supported mesic forest development. Importantly, recent studies highlight the role of fire refugia, topographic or edaphic features that protect forest patches within flammable landscapes, in maintaining and enabling the spread of fire-sensitive taxa such as *Podocarpus* and *Afrocarpus* (Beckett and Bond, 2019; Adie et al., 2017). Beckett and Bond (2019) propose that such refugia allow forest and savanna to persist as alternative stable states, while Adie et al. (2017) show that small rocky refugia in the Drakensberg act as long-term shelters for Afrotemperate forest species. These findings support the idea that *Podocarpus* could have used similar refugia along the humid coastal plain to persist and spread under favorable Mid-Holocene conditions. The climatic trends recorded in GeoB20615-2 are well supported by records at Braamhoek (Norström et al., 2009), Mfabeni (Miller et al., 2019). Mahwaqa (Neumann et al., 2014) and Lake Eteza (Neumann et al., 2010) where a phase of humidity after *c.* 7300 cal BP is obvious. As a driving factor, Miller et al. (2020) propose shifts in the southern hemispheric westerlies (SHW) and the associated South African high-pressure cell, that control the amount of moisture advection onto the continent.

During the Late Holocene after *c.* 3800 cal BP, the South African high-pressure cell shifted northward, in this position the high-pressure cell blocks tropical moisture in the central eastern region, causing the aridity trend (Miller et al., 2020; Chevalier and Chase, 2015). The Incomati catchment is at the northernmost extent of this region. The climate to the north/northwest is driven by insolation, and climate to the southwest is also driven by SHW shifts, but in the opposite sense since northwards shifts here induce a direct increase in rainfall by the westerly storm tracks (Miller et al., 2020). As a result, there are many apparent anomalies when comparing the GeoB20615-2 record with sites that are outside of the "central eastern zone" (compare Chevalier and Chase, 2015). The last *c.* 3800 years are in the Lake Eteza record and GeoB20615-2 characterised by a strong decrease of Podocarpaceae and other forest tree percentages. Overall, the close linkage between vegetation shifts at Delagoa Bight and at Lake Eteza shows a strong alignment between Indian Ocean coastal records pointing to similar environmental triggers. Since *c.* 2000 years the Lake Eteza region is affected by an increase of grasses and other open land indicators whereas the anthropogenic impact (*Pinus* pollen) is increasing towards the top of both records.

6. Conclusion

The continuous late Pleistocene-Holocene marine pollen record of GeoB20615-2 provides a novel reflection of terrestrial vegetation fluctuations for the eastern coast of Southern Africa, revealing key climate patterns over time although low sample resolution in some intervals limits interpretations. Key findings include a cool late Pleistocene period with strong presence of ericaceous shrubs from *c.* 16,600–15,000 cal BP. Climate variations inferred from pollen fluctuations correlate with sea level changes, including a major transgression *c.* 12,500–9000 cal BP that supported mangroves until drowning of the coastal landscape led to a decline of mangrove pollen in the sediments. During the early Holocene warming *c.* 11,500 cal BP cold-tolerant Ericaceae decreased further whereas savanna and forest taxa spread. The record aligns well with that of Lake Eteza since *c.* 10,300 cal BP. A middle Holocene humid phase (Holocene Altithermal) dominated by Podocarpaceae started *c.* 7700 cal BP, a dry period *c.* 3300 cal BP was marked by forest decline and a spread of Chenopodiaceae/Amaranthaceae. The observed climate variations correspond to those noted in the "central eastern zone" described by Miller et al. (2020), with the proposed climatic driver being the latitudinal shift of the South African high-pressure cell, which controls moisture advection onto the continent. At GeoB20615, the last *c.* 2500 years are affected by disturbances to unconsolidated sediments during coring. Although these disturbances obscure any possible pre-colonial anthropogenic impact, European influence is clearly visible from exotic pollen. The record, adding to a growing archive from the southeastern seaboard of Africa, demonstrates that marine sediments can capture land-based environmental changes even in a region of complex sediment redistribution such as Delagoa Bight. Despite complex transport and deposition processes affecting offshore sediment deposition, the marine pollen sequence shows good agreement with existing terrestrial records.

CRediT authorship contribution statement

F.H. Neumann: Writing – review & editing, Writing – original draft, Visualization, Validation, Resources, Methodology, Investigation, Formal analysis, Data curation, Conceptualization. **J. Finch:** Writing – review & editing, Writing – original draft, Validation, Methodology, Data curation, Conceptualization. **A. Hahn:** Writing – original draft, Methodology, Investigation, Formal analysis, Data curation. **C.S. Miller:** Writing – review & editing, Writing – original draft, Methodology, Formal analysis, Data curation. **L. Scott:** Writing – review & editing, Writing – original draft, Methodology, Investigation, Data curation. **E.**

Schefuß: Writing – review & editing, Methodology, Investigation, Data curation. **L. Dupont:** Writing – original draft, Validation, Methodology, Investigation. **H.C. Cawthra:** Writing – review & editing, Writing – original draft, Methodology, Investigation. **F. Engelbrecht:** Writing – review & editing, Writing – original draft, Methodology.

Declaration of competing interest

The authors declare that they have no known competing financial interests or personal relationships that could have appeared to influence the work reported in this paper.

Acknowledgements

Generous funding by PAST (Palaeontological Scientific Trust) enabled us to process the sediment samples for palynological analysis. Petrus Chakane processed the sediment samples at the palynological lab/Department of Plant Sciences, University of the Free State. Facilities at University of the Free State and at Evolutionary Studies Institute were used for pollen analysis. FHN was sponsored by a postdoctoral fellowship by University of KwaZulu-Natal from 2017 until April 2018. This work was financially supported by the Bundesministerium für Bildung und Forschung (BMBF, Bonn, Germany) within the project "Regional Archives for Integrated Investigation (RAiN)2". We thank the GeoB Core Repository at MARUM for providing the marine sample material and PANGAEA and Neotoma for archiving the data reported in this paper. We also thank the captain, the crew and scientists of the Meteor M123 cruise for recovering the studied material. Thank you to two anonymous reviewers as well as the Editor of Quaternary International, who helped improve the manuscript. We are grateful to Brice Gijsbertsen at the UKZN Cartographic Unit for professionally drafting Fig. 1.

Appendix A. Supplementary data

Supplementary data to this article can be found online at https://doi.org/10.1016/j.quaint.2025.109956.

Data availability

The data will be available via PANGAEA (https://www.pangaea.de) and the African Pollen Database component of Neotoma (www.neotomadb.org).

References

Adie, H., Kotze, J., Lawes, M.J., 2017. Small fire refugia in the grassy matrix and the persistence of afrotemperate forest in the Drakensberg Mountains. Sci. Rep. 7, 17421.

Armitage, S.J., Botha, G.A., Duller, G.A.T., Wintle, A.G., Rebêlo, L.P., Momade, F.J., 2006. The formation and evolution of the barrier islands of Incaha and Bazaruto, Mozambique. Geomorphology 82, 295–308.

Bamford, M.K., Neumann, F.H., Pereira, L.M., Scott, L., Dirks, P.H.G.M., Berger, L.R., 2010. Botanical remains from a coprolite from the Pleistocene hominin site of Malapa, Sterkfontein valley, South Africa. Palaeontol. Afr. 45, 23–28.

Bard, E., Rostek, F., Sonzogni, C., 1997. Interhemispheric synchrony of the last deglaciation inferred from alkenone palaeothermometry. Nature 385, 707–710.

Barker, S., Broecker, W., Clark, E., Hajdas, I., 2007. Radiocarbon age offsets of Foraminifera resulting from differential dissolution and fragmentation within the sedimentary bioturbated zone. Paleoceanography 22, PA2205. https://doi.org/10.1029/2006PA001354.

Beckett, H., Bond, W.J., 2019. Fire refugia facilitate forest and savanna co-existence as alternative stable states. J. Biogeogr. 46 (12), 2800–2810.

Bennett, K.D., 1996. Determination of the number of zones in a biostratigraphical sequence. New Phytol. 132, 155–170.

Blaauw, M., 2010. Methods and code for 'classical' age modelling of radiocarbon sequences. Quat. Geochronol. 5, 512–518.

Blaauw, M., Christen, J.A., 2011. Flexible paleoclimate age-depth models using an autoregressive gamma process. Bayesian Anal. 6, 457–474.

Bonnefille, R., Riollet, G., 1980. Pollens Des Savanes D'Afrique Orientale. Editions du Centre National de la Recherche Scientifique, Paris, p. 140, 113 pl.

Boon, R., 2010. Pooley's trees of eastern South Africa-a complete guide. Flora and Fauna Publication Trust c/o Natal Herbarium, p. 626. Durban.

Botha, G.A., 2018. Lithostratigraphy of the late Cenozoic Maputaland Group. S. Afr. J. Geol. 121, 95–108.

Botha, G.A., Scott, L., Vogel, J.C., von Brunn, V., 1992. Palaeosols and palaeoenvironments during the 'late Pleistocene hypothermal' in northern Natal. South Afr. J. Sci. 88, 508–512.

Bruton, M.N., Cooper, K.H. (Eds.), 1980. Studies on the Ecology of Maputaland. Rhodes University and Wildlife Society of South Africa. Grahamstown and, Durban, South Africa.

Burgess, N., Hales, J.D., Underwood, E., Dinerstein, E., Olson, D., Itousa, I., Schipper, J., Ricketts, T., Newman, K., 2004. The Terrestrial Ecoregions of Africa and Madagascar. Island Press, Washington DC, USA.

Burrows, J., Burrows, S., Lötter, M., Schmidt, E., 2018. Trees and Shrubs of Mozambique. Publishing Print Matters, Noordhoek, Cape Town, pp. 1–1114.

Chapman, L.J., Balirwa, J., Bugenyi, F.W.B., Chapman, C., Crisman, T.L., 2001. Wetlands of East Africa: biodiversity, exploitation, and policy perspectives. In: Gopal, B., Junk, W.J., Davis, J.A. (Eds.), Biodiversity in Wetlands: Assessment, Function and Conservation, 2. Backhuys Publishers, Leiden, pp. 101–131.

Chevalier, M., Chase, B.M., 2015. Southeast African records reveal a coherent shift from high- to low-latitude forcing mechanisms along the east African margin across the last glacial–interglacial transition. Quat. Sci. Rev. 125, 117–130.

Chevalier, M., Chase, B.M., Quick, L.J., Dupont, L.M., Johnson, T.C., 2020. Temperature change in subtropical southeastern Africa during the past 790,000 yr. Geology 49 (1), 71–75. https://doi.org/10.1130/G47841.1.

Chmura, G.L., Smirnov, A., Campbell, I.D., 1999. Pollen transport through distributaries and depositional patterns in coastal waters. Palaeogeogr. Palaeoclimatol. Palaeoecol. 149 (1–4), 257–270.

Coates Palgrave, M., 2002. Keith Coates Palgrave Trees of Southern Africa, third ed. Struik, Cape Town.

Coetzee, J.A., 1967. Pollen analytical studies in east and Southern Africa. Palaeoecol. Afr. 3, 1–146.

Cohen, A.S., 2003. Paleolimnology: the History and Evolution of Lake Systems. Oxford University Press, Oxford.

Cooper, J.A.G., Green, A.N., Compton, J.S., 2018. Sea-level change in Southern Africa since the last Glacial maximum. Quat. Sci. Rev. 201, 303–318.

Croudace, I.W., Rindby, A., Rothwell, R.G., 2015. Micro-XRF Studies of Sediment Cores: Applications of a Non-destructive Tool for the Environmental Sciences. Springer, Dordrecht.

Cushing, E.J., 1967. Evidence for differential pollen preservation in late Quaternary sediments in Minnesota. Rev. Palaeobot. Palynol. 4, 87–101.

Daru, B.H., van der Bank, M., Maurin, O., Yessoufou, K., Schaefer, H., Slingsby, J.A., Davies, T.J., 2016. A novel phylogenetic regionalization of phytogeographical zones of southern Africa reveals their hidden evolutionary affinities. J. Biogeogr. 43 (1), 155–166.

De Lecea, A.M., Green, A.N., Cooper, J.A.G., Strachan, K.L., Wiles, E.A., 2017. Stepped Holocene sea-level rise and its influence on sedimentation in a large marine embayment: Maputo Bay, Mozambique. Estuarine. Coast. Shelf Sci. 193, 25–36.

Dupont, L.M., Kuhlmann, H., 2017. Glacial-interglacial vegetation change in the Zambezi catchment. Quat. Sci. Rev. 155, 127–135.

Dupont, L.M., Behling, H., Jahns, S., Marret, F., Kim, J.-H., 2007. Variability in glacial and Holocene marine pollen records offshore from west southern Africa. Veg. Hist. Archaeobotany 16, 87–100.

Dupont, L., Caley, T., Kim, J.-H., Castañeda, I.S., Malaizé, B., Giraudeau, J., 2011. Glacial-interglacial vegetation dynamics in South Eastern Africa coupled to sea surface temperature variations in the Western Indian Ocean. Clim. Past 7, 1209–1224.

Dyer, S.E., Green, A.N., Cooper, J.A.G., Hahn, A., Zabel, M., 2021. Response of a wave-dominated coastline and delta to antecedent conditioning and fluctuating rates of postglacial sea-level rise. Mar. Geol. 434, 106435.

Eeley, H.A.C., Lawes, M.J., Piper, S.E., 1999. The influence of climate change on the distribution of indigenous forest in KwaZulu-Natal, South Africa. J. Biogeogr. 26, 595–617.

Effiom, A.C., Neumann, F.H., Bamford, M.K., Scott, L., 2024. Mid-late Holocene palynological development at Lake St Lucia, KwaZulu-Natal. Rev. Palaeobot. Palynol. 322, 105046.

Effiom, A.C., Neumann, F.H., Scott, L., Bamford, M.K., 2025. Morphology and ecological significance of Holocene palynomorphs from the Indian Ocean coastal belt biome of South Africa. Palynology. https://doi.org/10.1080/01916122.2024.24.

Ekblom, A., 2008. Forest-savanna dynamics in the coastal lowland of southern Mozambique since c. AD 1400. Holocene 18 (8), 1247–1257.

Ekblom, A., Risberg, J., Holmgren, K., 2014a. Coastal forest and miombo woodland history of the Vilankulo region, Mozambique. Holocene 24 (3), 284–294.

Ekblom, A., Eichhorn, B., Sinclair, P., Badenhorst, S., Berger, A., 2014b. Land use history and resource utilisation from A.D. 400 to the present, at Chibuene, southern Mozambique. Veg. Hist. Archaeobotany 23, 15–32.

Ellison, J.C., 1993. Mangrove retreat with rising sea-level Bermuda. Estuar. Coast. Shelf Sci. 37, 75–87.

Engelbrecht, C.J., Engelbrecht, F.A., 2016. Shifts in köppen-geiger climate zones over Southern Africa in relation to key global temperature goals. Theor. Appl. Climatol. 123, 247–261.

Engelbrecht, F.A., Adegoke, J., Bopape, M.J.M., Naidoo, M., Garland, R., Thatcher, M., McGregor, J., Katzfey, J., Werner, M., Ichoku, C., 2015. Projections of rapidly rising surface temperatures over Africa under low mitigation. Environ. Res. Lett. 10, 085004.

Erdtman, G., 1957. Pollen and spore morphology/plant taxonomy. In: Gymnospermae, Pteridophyta Bryophyta. Almqvist and Wiksell, Stockholm, pp. 5–44. Chap. 2.

Fægri, K., Iversen, J., 1989. Textbook of Pollen Analysis, fourth ed. John Wiley and Sons, Chichester.
Felton, I., 1998. Illegal swamp forest destruction in the KwaZibi and Mnyayiza areas of the Kosi Bay coastal forest reserve. KwaZulu-Natal Nature Conservation Service. Pietermaritzburg. Unpublished Report.
Fietz, S., Baker, A., Miller, C.S., Naafs, D.A., Peterse, F., Finch, J., Humphries, M., Schefuß, E., Roychoudhury, A.N., Routh, J., 2023. Terrestrial temperature evolution of southern Africa during the late Pleistocene and Holocene: evidence from the Mfabeni peatland. Quat. Sci. Rev. 299, 107870.
Finch, J.M., Hill, T.R., 2008. A late Quaternary pollen sequence from Mfabeni peatland, South Africa: reconstructing forest history in Maputaland. Quat. Res. 70, 442–450.
Förster, R., 1975. The geological history of the sedimentary basin of southern Mozambique, and some aspects of the origin of the Mozambique channel. Palaeogeogr. Palaeoclimatol. Palaeoecol. 17 (4), 267–287.
Govin, A., Holzwarth, U., Heslop, D., Ford Keeling, L., Zabel, M., Mulitza, S., Chiessi, C. M., 2012. Distribution of major elements in Atlantic surface sediments (36°N–49°S): imprint of terrigenous input and continental weathering. G-cubed 13 (1), Q01013.
Grimm, E.C., 1987. CONISS: a FORTRAN 77 program for stratigraphically constrained cluster analysis by the method of incremental sum of squares. Comput. Geosci. 13, 13–35.
Grimm, E.C., 1992. Tilia and Tilia-graph: pollen spreadsheet and graphics programs. Programs and Abstracts, 8th International Palynological Congress, Aix-en-Provence 56. September 6-12.
Hahn, A., Schefuß, E., Andò, S., Cawthra, H.C., Frenzel, P., Kugel, M., Meschner, S., Mollenhauer, G., Zabel, M., 2017. Southern hemisphere anticyclonic circulation drives oceanic and climatic conditions in late Holocene southernmost Africa. Clim. Past 13, 649–665.
Hahn, A., Miller, C., Andó, S., Bouimetarhan, I., Cawthra, H.C., Garzanti, E., Green, A., Radeff, G., Schefuß, E., Zabel, M., 2018. The provenance of terrigenous components in marine sediments along the east Coast of Southern Africa. G-cubed 19. https://doi.org/10.1029/2017GC007228.
Hamilton, A.C., 1972. The interpretation of pollen diagrams from highland Uganda. Palaeoecol. Afr. 7, 45–149.
Havinga, A.J., 1967. Palynology of pollen preservation. Rev. Palaeobot. Palynol. 2, 81–98.
Hogg, A.G., Heaton, T.H., Hua, Q., Palmer, J.G., Turney, C.S.M., Southon, J., Bayliss, A., Blackwell, P.G., Boswijk, Bronk, Ramsey, C., Pearson, C., Petchey, F., Reimer, P., Reimer, R., Wacker, L., 2020. SHCal20 southern hemisphere calibration, 0-55,000 years cal BP. Radiocarbon 62 (4), 759–778.
Hooghiemstra, H., Lézine, A.-M., Leroy, S.A.G., Dupont, L.M., Marret, F., 2006. Late Quaternary palynology in marine sediments: a synthesis of the understanding of pollen distribution patterns in the NW African setting. Quat. Int. 148, 29–44.
Hopkins, J.A., McCarthy, F.M.G., 2002. Post-depositional palynomorph degradation in Quaternary shelf sediments: a laboratory experiment studying the effects of progressive oxidation. Palynology 26, 167–184.
IPCC, 2021. Climate Change 2021: the Physical Science Basis. Contribution of Working Group I to the Sixth Assessment Report of the Intergovernmental Panel on Climate Change. Cambridge University Press, Cambridge, United Kingdom and New York, NY, USA, p. 2391. https://doi.org/10.1017/9781009157896.
Köppen, W., 1936. Das Geographisches System der Klimate. In: Koppen, W., Geiger, R. (Eds.), Handbuch Der Klimatologie I(C). Gebrueder Borntraeger, Berlin.
Kotze, D.C., O'Connor, T.G.O., 2000. Vegetation variation within and among palustrine wetlands along an altitudinal gradient in KwaZulu-Natal, South Africa. Plant Ecol. 146, 77–96, 2000.
Krauss, K.W., Lovelock, C.E., McKee, K.L., Lopez-Hoffman, L., Ewe, S.M., Sousa, W.P., 2008. Environmental drivers in mangrove establishment and early development: a review. Aquat. Bot. 89, 105–127.
Lamont, T., Roberts, M.J., Barlow, R.G., Morris, T., van den Berg, M.A., 2010. Circulation patterns in the Delagoa Bight, Mozambique, and the influence of deep ocean eddies. Afr. J. Mar. Sci. 32, 553–562.
Lawes, M.J., 1990. The distribution of the samango monkey (*Cercopithecus mitis erythrarchus* Peters, 1852 and *Cercopithecus mitis labiatus* l. Geoffroy, 1843) and forest history in South Africa. J. Phylogeograph. 17, 669–680.
Lawes, M.J., Mealin, P.E., Piper, S.E., 2000a. Patch occupancy and potential metapopulation dynamics of three forest mammals in fragmented afromontane forest in South Africa. Conserv. Biol. 14, 1088–1098.
Lawes, M.J., Eeley, H.A.C., Piper, S.E., 2000b. The relationship between local and regional diversity of Indigenous forest fauna in KwaZulu-Natal province, South Africa. Biodivers. Conserv. 9, 683–705.
Lawes, M.J., Eeley, H.A.C., Findlay, N.J., Forbes, D., 2007. Resilient forest faunal communities in South Africa: a legacy of palaeoclimatic change and extinction filtering? J. Biogeogr. 34, 1246–1264.
Lencart, e Silva J.D., Simpson, J.H., Hoguane, A.M., Harcourt-Baldwin, J.-L., 2010. Buoyancy-stirring interactions in a subtropical embayment: a synthesis of measurements and model simulations in Maputo Bay, Mozambique. Afr. J. Mar. Sci. 32, 95–107.
Low, A.B., Rebelo, A.G., 1996. Vegetation of South Africa, Lesotho and Swaziland. Department of Environmental Affairs and Tourism, Pretoria, South Africa.
Lubbe, R.A., 1997. Vegetation and flora of the Kosi Bay coastal forest reserve in Maputaland, northern KwaZulu-Natal, South Africa. M.Sc. Thesis Department of Botany. University of Pretoria.
Lutjeharms, J.R., 2006. The coastal oceans of south-eastern Africa. In: Robinson, A.R., Brink, K.H. (Eds.), The Global Coastal Ocean: Regional Studies and Syntheses (The Sea: Ideas and Observations on Progress in the Study of the Seas Volume 14 Part B. Harvard University Press, Cambridge, Mass, pp. 783–834.
Maboya, M.L., Meadows, M.E., Reimer, P.J., Backeberg, B.C., Haberzettl, T., 2017. Late Holocene marine radiocarbon reservoir correction for the southern and eastern coasts of South Africa. Radiocarbon 60, 571–582.
Mavume, A., Pinto, I., Massuanganhe, E., 2014. Potential climate change impacts on Maputo Bay. In: Bandeira, S., Paula, J. (Eds.), The Maputo Bay Ecosystem. WIOMSA, Zanzibar Town, pp. 383–397.
Mazus, H., 2000. Clues on the history of *Podocarpus* forest in Maputaland, South Africa, during the Quaternary, based on pollen analysis. Afr. Geosci. Rev. 7, 75–82.
Mercuri, A.M., D'Andrea, A.C., Fornaciari, R., Höhn, A., 2018. Plants and People in the African Past: Progress in African Archaeobotany. Springer, Berlin/Heidelberg, Germany.
Miller, C., Finch, J., Hill, T., Peterse, F., Humphries, M., Zabel, Z., Schefuß, E., 2019. Late Quaternary climate variability at Mfabeni peatland, eastern South Africa. Clim. Past 15, 1153–1170.
Miller, C., Hahn, A., Liebrand, D., Zabel, M., Schefuß, E., 2020. Mid- and low latitude effects on eastern South African rainfall over the Holocene. Quat. Sci. Rev. 229, 106088.
Moll, E.J., White, F., 1978. The Indian Ocean coastal belt. In: WERGER, M.J.A. (Ed.), Biogeography and Ecology of Southern Africa, pp. 561–598. W. Junk, The Hague.
Mucina, L., Rutherford, M., 2006. The vegetation of South Africa, Lesotho and Swaziland. In: Memoirs of the Botanical Survey of South Africa, Strelitzia, 19. South African National Biodiversity Institute, Pretoria.
Mucina, L., Scott-Shaw, C.R., Rutherford, M.C., Camp, K.G.T., Matthews, W.S., Powrie, L. W., Hoare, D.B., 2006. Indian Ocean coastal belt. In: Mucina, L., Rutherford, M.C. (Eds.), The Vegetation of South Africa, Lesotho and Swaziland, Strelitzia 19. South African National Biodiversity Institute, Pretoria, pp. 569–583.
Mussa, A., Mugabe, J., Cuamaba, F., Haldorsen, S., 2003. Late Weichselian to Holocene evolution of the Maputo Bay, Mozambique. XVI International Union for Quaternary Research (INQUA) Congress. INQUA, Reno, NV.
Nakayama, M., 2003. International Waters in Southern Africa. United Nations University Press, p. 9.
Neumann, F.H., Stager, J., Scott, L., Hendrik, J., Weyhenmeyer, C., 2008. Holocene vegetation and climate records from Lake Sibaya, KwaZulu-Natal (South Africa). Rev. Palynol. Palaeobotany 152, 113–128.
Neumann, F.H., Scott, L., Bousman, C., Van As, L., 2010. A Holocene sequence of vegetation change at Lake Eteza, coastal KwaZulu-Natal, South Africa. Rev. Palaeobot. Palynol. 162, 39–53.
Neumann, F.H., Botha, G.A., Scott, L., 2014. 18,000 years of grassland evolution in the summer rainfall region of South Africa: evidence from Mahwaqa Mountain, KwaZulu-Natal. Veg. Hist. Archaeobotany 23 (6), 665–681.
Niang, I., Ruppel, O.C., Abdrabo, M.A., Essel, A., Lennard, C., Padgham, J., Urquhart, P., 2014. Africa. In: Barros, V.R., Field, C.B., Dokken, D.J., Mastrandrea, M.D., Mach, K. J., Bilir, T.E., Chatterjee, M., Ebi, K.L., Estrada, Y.O., Genova, R.C., Girma, B., Kissel, E.S., Levy, A.N., MacCracken, S., Mastrandrea, P.R., White, L.L. (Eds.), Climate Change 2014: Impacts, Adaptation, and Vulnerability. Part B: Regional Aspects. Contribution of Working Group II to the Fifth Assessment Report of the Intergovernmental Panel on Climate Change. Cambridge University Press, Cambridge, United Kingdom and New York, NY, USA, pp. 1199–1265.
Norström, E., Scott, L., Partridge, T.C., Risberg, J., Holmgren, K., 2009. Reconstruction of environmental and climate changes at Braamhoek wetland, eastern escarpment South Africa, during the last 16,000 years with emphasis on the Pleistocene–Holocene transition. Palaeogeogr. Palaeoclimatol. Palaeoecol. 271, 240–258.
Norström, E., Risberg, J., Gröndahl, H., Holmgren, K., Snowball, I., Mugabe, J.A., Sitoe, S.R., 2012. Coastal paleo-environment and sea-level change at Macassa Bay, southern Mozambique, since c 6600 cal BP. Quat. Int. 260, 153–163.
Norström, E., Neumann, F.H., Scott, L., Smittenberg, R.H., Holmstrand, H., Lundqvist, S., Snowball, I., Sundqvist, H.S., Risberg, J., Bamford, M., 2014. Late Quaternary vegetation dynamics and hydro-climate in the Drakensberg, South Africa. Quat. Sci. Rev. 105, 48–65.
Olatoyan, J., Neumann, F.H., Orijemie, E.A., Sievers, C., Evans, M., Mvelase, S., Hattingh, T., Schoeman, A.M.H., 2022. Archaeobotanical evidence for the emergence of pastoralism and farming in Southern Africa. Acta Palaeobot. 62 (1), 50–75.
Olson, D.M., Dinerstein, E., Wikramanayake, E.D., Burgess, N.D., Powell, G.V.N., Underwood, E.C., D'amico, J.A., Itoua, I., Strand, H.E., Morrison, J.C., Loucks, C.J., Allnutt, T.F., Ricketts, T.H., Kura, Y., Lamoreux, J.F., Wettengel, W.W., Hedao, P., Kassem, K.R., 2001. Terrestrial ecoregions of the worlds: a new map of life on Earth. Bioscience 51, 933–938.
Partridge, T.C., Scott, L., Hamilton, J.E., 1999. Synthetic reconstructions of southern African environments during the last glacial maximum (21-18 kyr) and the Holocene Altithermal (8-6 kyr). Quat. Int. 57 (/58), 207–214.
Pedro, J., Bostock, H., Bitz, C., He, F., Vandergoes, M.J., Steig, E.J., Chase, B.M., Krause, C.E., Rasmussen, S.O., Markle, B.R., Cortese, G., 2016. The spatial extent and dynamics of the antarctic cold reversal. Nat. Geosci. 9, 51–55.
Phuphumirat, W., Zetter, R., Hofmann, C.-C., Ferguson, D.K., 2015. Pollen degradation in mangrove sediments: a short-term experiment. Rev. Palaeobot. Palynol. 221, 106–116.
Preu, B., Spieß, V., Schwenk, T., Schneider, R., 2011. Evidence for current-controlled sedimentation along the southern Mozambique Continental margin since early Miocene times. Geo Mar. Lett. 31, 427–435.
Raynaud, D., Barnola, J.-M., Chapellaz, J., Blunier, T., Inedermuhle, A., Stauffer, B., 2000. The ice core record of greenhouse gasses: a view in the context of future changes. Quat. Sci. Rev. 19, 9–17.
Reason, C.J.C., 2001. Subtropical Indian Ocean SST dipole events and southern African rainfall. Geophys. Res. Lett. 28, 2225–2227.

Renssen, H., Seppä, H., Crosta, X., 2012. Global characterization of the Holocene Thermal Maximum. Quat. Sci. Rev. 48, 7–19.
Scheffers, B.R., De Meester, L., Bridge, T.C.L., Hoffmann, A.A., Pandolfi, J.M., Corlett, R. T., Butchart, S.H.M., Pearce-Kelly, P., Kovacs, K.M., Dudgeon, D., Pacifici, M., Rondinini, C., Foden, W.B., Martin, T.G., Mora, C., Bickford, D., Watson, J.E.M., 2016. The broad footprint of climate change from genes to biomes to people. Science 354, 6313 aaf7671.
Schüürman, J., Hahn, A., Zabel, M., 2019. In search of sediment deposits from the Limpopo (Delagoa Bight, southern Africa): deciphering the catchment provenance of coastal sediments. Sediment. Geol. 380, 94–104.
Scott, L., 1982. Late Quaternary fossil pollen grains from the Transvaal, South Africa. Rev. Palaeobot. Palynol. 36 (3–4), 241–278.
Scott, L., 2016. Fluctuations of vegetation and climate over the last 75 000 years in the savanna biome, South Africa: Tswaing Crater and wonderkrater pollen sequences reviewed. Quat. Sci. Rev. 145, 117–133.
Scott, L., Thackeray, J.F., 1987. Multivariate analysis of late Pleistocene and Holocene pollen spectra from Wonderkrater, Transvaal, South Africa. South Afr. J. Sci. 83, 93–98.
Scott, L., Holmgren, K., Talma, A.S., Woodborne, S., Vogel, J.C., 2003. Age interpretation of the Wonderkrater spring sediments and vegetation change in the savanna biome, Limpopo province, South Africa. South Afr. J. Sci. 99 (9), 484–488.
Scott, L., Neumann, F.H., Brook, G., Bousman, C., Norström, E., Metwally, A., 2012. Terrestrial Fossil-pollen evidence of climate change during the last 26 thousand years in Southern Africa. Quat. Sci. Rev. 32, 100–118.
Sefton, J.P., Woodroffe, S.A., 2021. Assessing the use of mangrove pollen as a quantitative sea-level indicator on Mahé, Seychelles. J. Quat. Sci. 36 (2), 311–323. https://doi.org/10.1002/jqs.3272.
Sell, A.F., von Maltitz, G.P., Auel, H., Biastoch, A., Bode-Dalby, M., Brandt, P., Duncan, S. E., Ekau, W., Fock, H.O., Hagen, W., Huggett, J.A., Koppelmann, R., Körner, M., Lahajnar, N., Martin, B., Midgley, G.F., Rixen, T., van der Lingen, C.D., Verheye, H. M., Wilhelm, M.R., 2024. Chapter 2: unique southern African terrestrial and oceanic biomes and their relation to steep environmental gradients. In: von Maltitz, G.P., et al. (Eds.), Sustainability of Southern African Ecosystems Under Global Change, Ecological Studies, 248. Springer Open Access, pp. 23–88.
Siebert, S.J., Fish, L., Uiras, M.M., Izidine, S.A., 2004. Grass assemblages and diversity of conservation areas on the coastal plain south of Maputo Bay, Mozambique. Bothalia 34, 61–71.
Simon, M.H., Ziegler, M., Bosmans, J., Barker, S., Reason, C.J.C., Hall, I.R., 2015. Eastern South African hydroclimate over the past 270,000 years *science reports*, 5, 18153.
Stager, J.C., Ryves, D.B., King, C., Madson, J., Hazzard, M., Neumann, F.H., Maud, R.R., 2013. Late Holocene precipitation variability in the summer rainfall region of South Africa. Quat. Sci. Rev. 67, 105–120.
Steenkamp, Y., van Wyk, A.E., Victor, J.E., Hoare, D.B., Smith, G.F., 2004. Maputaland–pondoland–albany. In: Mittermeier, R.A., Robles Gil, P., Hoffmann, M., Pilgrim, J., Brooks, T., Mittermeier, C.G., Lamoreux, J., Fonseca, G.A.B. (Eds.), Hotspots Revisited: Earth's Biologically Richest and Most Endangered Terrestrial Ecoregions. CEMEX, Mexico City, pp. 219–228.
Thackeray, J.F., Scott, L., Pieterse, P., 2019. The younger Dryas interval at Wonderkrater (South Africa) in the context of a platinum anomaly. Palaeontol. Afr. 54, 30–35.
Tyson, R.V., 1995. Sedimentary Organic Matter-Organic Facies and Palynofacies. Chapman and Hall, London, p. 615.
van Wyk, A.E., 1994. Maputaland-pondoland region. In: Davis, S.D., Heywood, V.H., Hamilton, A.C. (Eds.), Centres of Plant Diversity, a Guide and Strategy for their Conservation, 1. Information Press, Oxford, pp. 227–235.
van Wyk, A.E., Smith, G.F., 2001. Regions of Floristic Endemism in Southern Africa: a Review with Emphasis on Succulents. Umdaus Press, Pretoria.
Venter, H.J.T., 1972. *Die Plantekologie Van Richardsbaai, Natal.* D.Sc. Thesis, Dept of Botany. University of Pretoria.
Vesey-Fitzgerald, D.F., 1970. The origin and distribution of valley grasslands in East Africa. J. Ecol. 58, 51–75.
Walther, S., Neumann, F., 2011. Sedimentology, isotopes and palynology of late Holocene cores from Lake sibaya and the Kosi Bay system (KwaZulu- Natal, South Africa). S. Afr. Geogr. J. 93 (2), 133–153.
White, F., 1983. The Vegetation of Africa: a Descriptive Memoir to Accompany the UNESCO/AETFAT/UNSO Vegetation Map of Africa Natural Resources Research, 20. UNESCO, Paris, France.
Wild, H., Grandvaux Barbosa, L.A., 1967. Vegetation map (1:2,500. 000 in Colour) of the Flora Zambesiaca Area, Descriptive Memoir. Supplement to Flora Zambesiaca. M.O. Collins Ltd., Salisbury.
Zabel, M., 2016. Climate Archives in Coastal Waters of Southern Africa (Meteor Berichte). Cruise No. M123.
Zinke, J., Dullo, W.C., Heiss, G.A., Eisenhauer, A., 2004. ENSO and Indian Ocean subtropical dipole variability is recorded in a coral record off southwest Madagascar for the period 1659 to 1995. Earth Planet Sci. Lett. 228 (1–2), 177–194.